

CHAPTER 6

Conductivity, Electrical Switching, Thermoelectric Power Studies

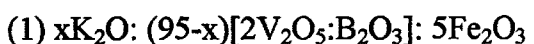
CHAPTER –6

6.1 ELECTRICAL CONDUCTIVITY STUDIES:

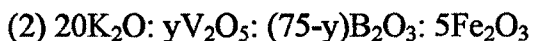
6.11 INTRODUCTION:

Electrical conductivity studies of oxide glasses having semiconducting nature were carried out by many workers and suggested that the carrier mechanism is due to small polarons. ^[1-7]

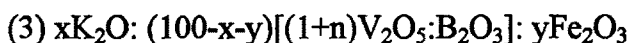
Electrical conductivity studies have been carried out on the following series of the glass samples.



where $x=0$ to 30 in step of 5 mole %.



where $y=40$ to 75 in step of 5 mole %.



where $x=0$ to 20 in step of 5 mole %.

$y=5$ to 15 mole % in step of 2.5 mole %.

$n = 0.2$ to 1 in step of 0.2.

On the basis of Mott's theory the conduction mechanism has been discussed in present glass systems.

6.12 SEMICONDUCTING NATURE:

Of the transition metal oxides, which cause semiconductivity in glasses, V_2O_5 is unique by being itself as a glass former. Thus, glasses containing V_2O_5 are of great interest for studying the correlation between electrical properties and glass network structure. A number of works have been published on glasses containing V_2O_5 ^[1,2,4,6-8]. In the present work, the effect

of glass modifier K_2O , glass formers B_2O_3 and V_2O_5 on conductivity and activation energy has been discussed.

The dc conductivity of the present glasses containing transition metal oxide can be expressed by ^[9-10]

$$\sigma = \frac{\nu_o e^2 c(1-c)}{kTR} \exp(-2\alpha R) \exp(-W/kT) \quad (6.11)$$

where ν_o is the optical phonon frequency which is assumed as $\approx 10^{13}$ Hz^[10] for the present glass system. c is the mole fraction of the site occupancy by electron. For the V_2O_5 based glasses c is V^{+4}/V_{total} ^[10], e is the electronic charge, α is the electron wave function decay constant. The fraction of reduced V ions to the total V ions [$c=V^{+4}/V_{total}$] was calculated by the chemical analysis (Chapter 3.6)^[11]. The values of c obtained from the chemical analysis are shown in Table 6.11. The value of c for all three glass series are found to increase with the decrease of the V_2O_5 amount. A similar result was also made by Ghosh et. al^[12] for V_2O_5 - Bi_2O_3 glass system. W , the activation energy was calculated by computer fitting the curve between $\log \sigma$ and $10^3/T$ [Figure 6.11 (a), (b) and (c)] for all three glass series.

The results of the conductivity measurements as a function of temperature in the range 315-433 °K for all different compositions are shown in Figure 6.11(a), (b) and (c). The general behaviour of the curve are similar to that reported for V_2O_5 - P_2O_5 glasses ^[6-7,13], V_2O_5 - TeO_2 ^[14], WO_3 - P_2O_5 ^[15]. The log of dc conductivity at any given composition increases linearly with $10^3/T$ temperature. According to Arrheneous equation^[3,9],

$$\sigma = \sigma_o \exp(-W/kT) \quad (6.12)$$

It has been observed from Figure 6.11 (a) that the decrease in the conductivity at 100 °C upto 10 mole % of K_2O is 64 % and from 15 mole % to 30 mole % of K_2O , the conductivity decreases by 96 %. In the second series Figure 6.11(b), upto 60 mole % of V_2O_5 , the conductivity increases by 92 % and above 60 mole % of V_2O_5 , the conductivity increase by 76 %, whereas in

Table 6.11 : Electrical Conductivity data of Series 1, 2 and 3.

Series	Mole %	W (eV)	W _H (eV)	v _p (Å)	α'	V ³⁺ 10 ²⁰	V ³⁺ N _{total}	V-V spacing (Å)	α (Å) ⁻¹	J	$\left(\frac{2kT W_H}{\pi}\right)^{1/4} \left(\frac{h v_0}{\pi}\right)^{1/2}$	σ ₁₀₀ Ω ⁻¹ Cm ⁻¹
Series 1	K ₂ O=0 %	0.407	0.327	1.67	0.0119	2.14	0.0154	4.16	4.99	0.0689	0.0124	1.59 x 10 ⁻⁵
	5	0.411	0.332	1.68	0.0232	2.96	0.0216	4.18	4.86	0.0729	0.0125	3.55 x 10 ⁻⁶
	10	0.420	0.336	1.70	0.0116	3.19	0.0239	4.22	4.78	0.0819	0.0125	5.62 x 10 ⁻⁶
	15	0.442	0.339	1.72	0.0336	3.24	0.0256	4.27	4.68	0.1039	0.0126	1.59 x 10 ⁻⁶
	20	0.479	0.342	1.74	0.0579	3.91	0.0317	4.33	4.72	0.1409	0.0126	5.62 x 10 ⁻⁷
	25	0.509	0.347	1.76	0.0504	3.98	0.0332	4.37	4.58	0.1709	0.0126	4.47 x 10 ⁻⁷
	30	0.536	0.343	1.82	0.0848	4.16	0.0385	4.52	4.39	0.1979	0.0126	2.04 x 10 ⁻⁷
Series 2	V ₂ O ₅ =40 %	0.585	0.327	1.975	0.0361	8.17	0.096	4.90	4.05	0.255	0.0124	1.78 x 10 ⁻⁸
	45	0.572	0.337	1.843	0.0472	7.90	0.0756	4.57	4.34	0.242	0.0125	2.51 x 10 ⁻⁸
	50	0.556	0.340	1.756	0.0464	6.88	0.0570	4.36	4.59	0.226	0.0126	3.39 x 10 ⁻⁸
	55	0.522	0.336	1.716	0.0261	5.36	0.0414	4.26	4.80	0.192	0.0125	1.29 x 10 ⁻⁷
	60	0.512	0.333	1.665	0.0394	4.67	0.0329	4.13	4.84	0.183	0.0125	2.40 x 10 ⁻⁷
	65	0.501	0.327	1.635	0.0221	3.56	0.0238	4.06	4.97	0.172	0.0125	4.47 x 10 ⁻⁷
	70	0.459	0.321	1.609	0.0470	3.39	0.0216	3.99	5.08	0.130	0.0124	6.31 x 10 ⁻⁷
Series 3	75	0.451	0.315	1.583	0.0365	2.59	0.0157	3.93	5.28	0.122	0.0123	1.00 x 10 ⁻⁶
	Fe ₂ O ₃ =5 %	0.410	0.343	1.738	0.0232	2.58	0.0207	4.31	4.67	0.083	0.0126	2.40 x 10 ⁻⁶
	7.5	0.431	0.334	1.746	0.0397	2.79	0.0226	4.33	4.65	0.104	0.0125	8.59 x 10 ⁻⁷
	10	0.455	0.327	1.760	0.0463	3.03	0.0252	4.37	4.60	0.128	0.0124	5.13 x 10 ⁻⁷
	12.5	0.496	0.319	1.788	0.0579	3.20	0.0279	4.44	4.51	0.169	0.0124	2.00 x 10 ⁻⁷
	15	0.506	0.313	1.820	0.0695	3.40	0.0313	4.52	4.39	0.179	0.0123	7.94 x 10 ⁻⁸

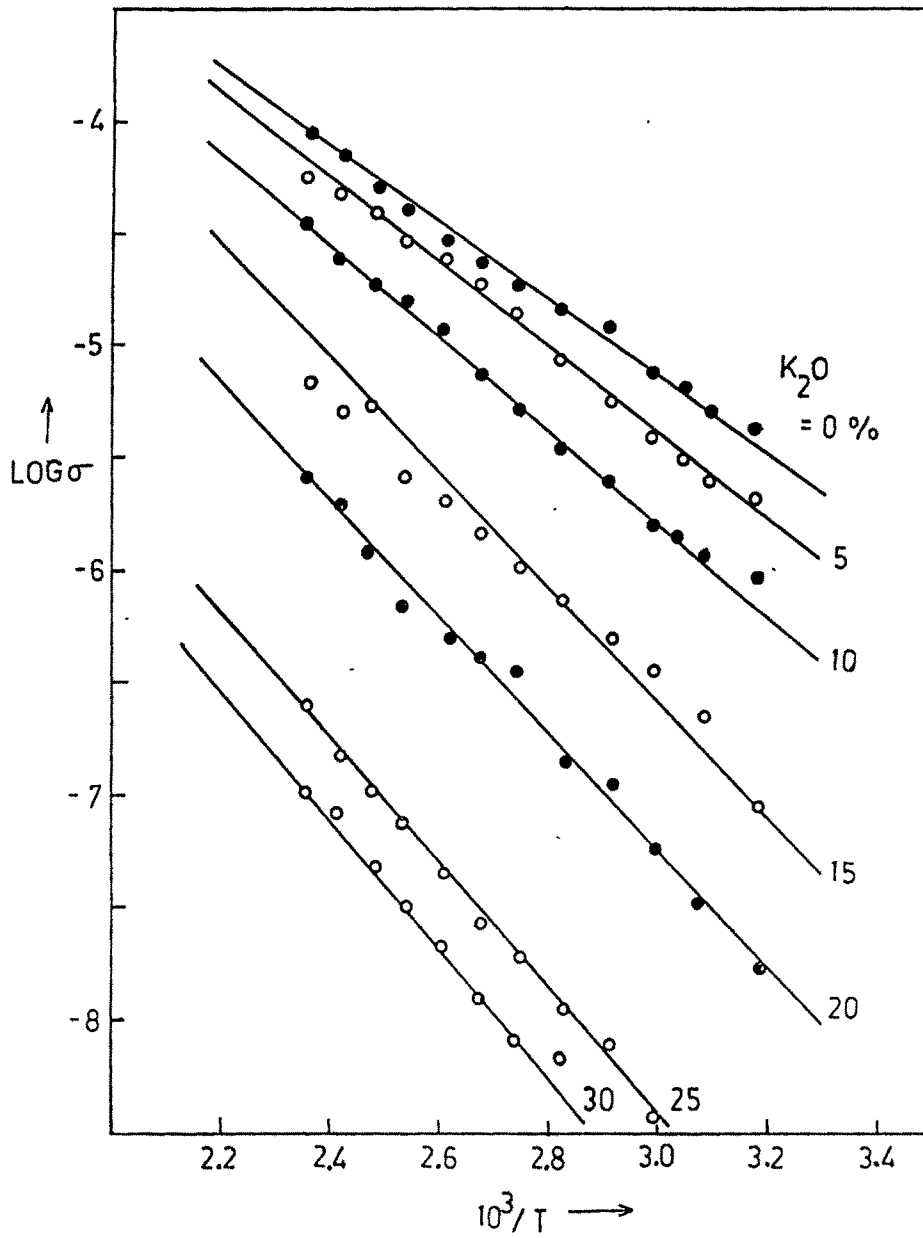


Figure 6.11 (a) : Plot of $\text{Log } \sigma$ versus $10^3/T$ for series 1.

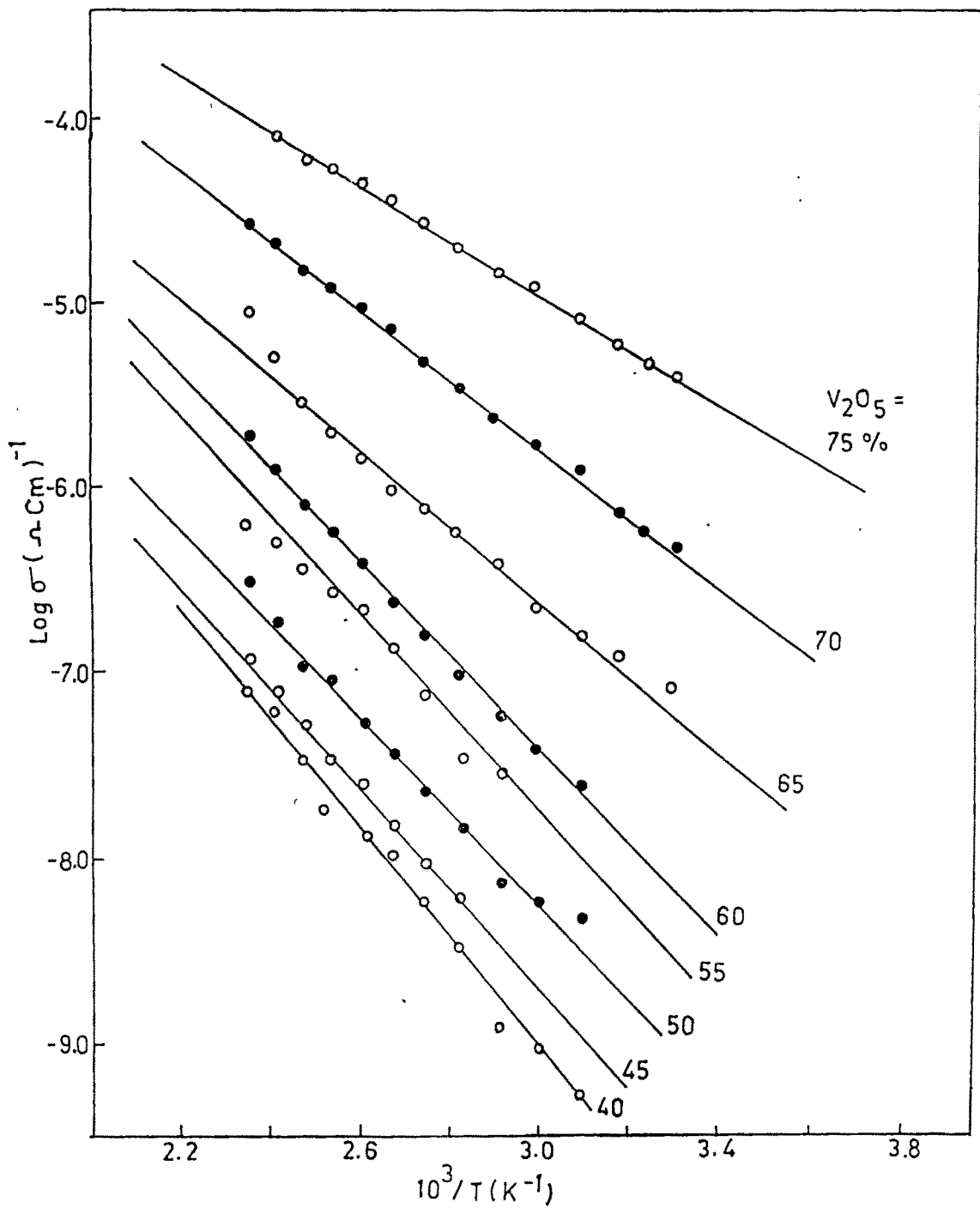


Figure 6.11 (b) : Plot of $\text{Log } \sigma$ versus $10^3/T$ for series 2.

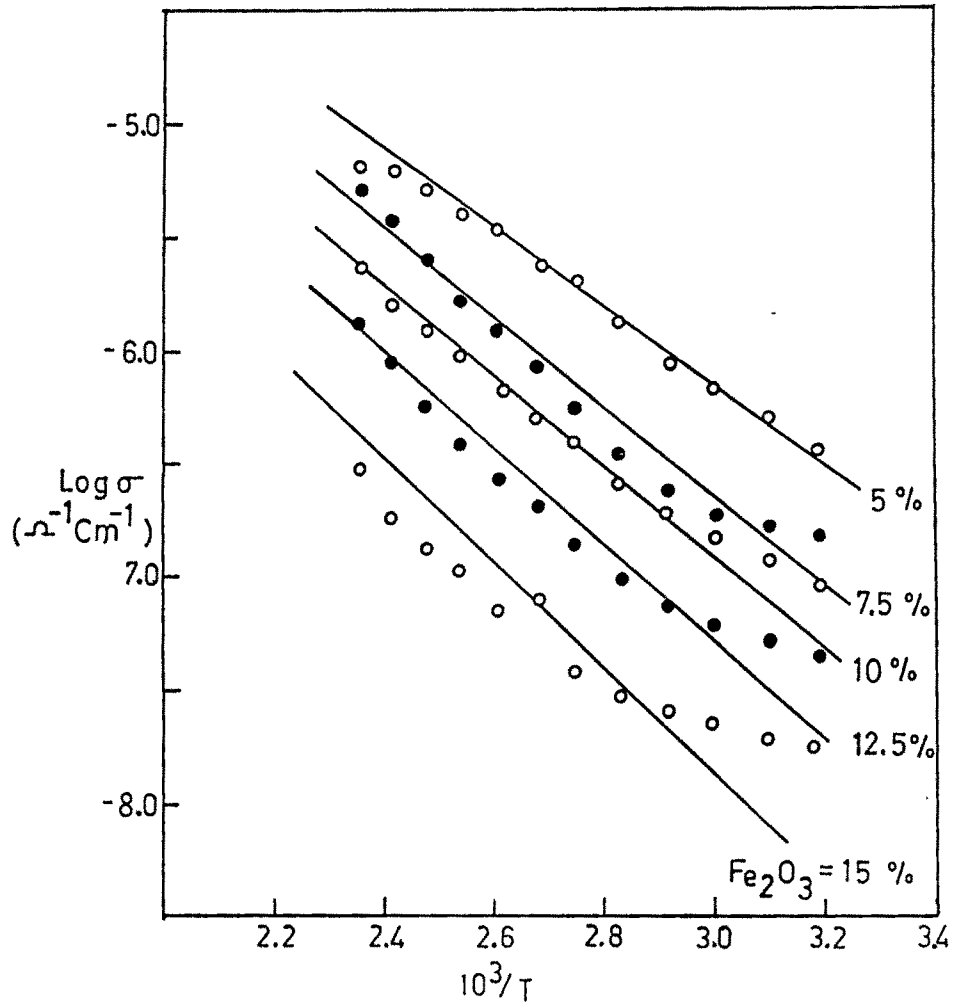


Figure 6.11 (c) : Plot of $\text{Log } \sigma$ versus $10^3/T$ for series 3.

series-3, Figure 6.11(c), the conductivity decreases linearly for $\text{Fe}_2\text{O}_3 = 5$ to 20 mole %. Variation of conductivity is observed in all three series from 10^{-5} to $10^{-8} \Omega^{-1}\text{cm}^{-1}$ and $\log\sigma$ vs $10^3/T$ is linear, which shows the semiconducting behaviour of the present glass series. The n-type semiconducting nature of these glasses has been confirmed by seebeck measurement (Section 6.3)^[16]. Mori and H. Sakata^[17-18] reported $\text{V}_2\text{O}_5\text{-Sb}_2\text{O}_3\text{-TeO}_2$ and $\text{V}_2\text{O}_5\text{-Bi}_2\text{O}_3\text{-TeO}_2$ glasses as a n-type semiconductor.

6.13 SMALL POLARON HOPPING:

A small polaron theory has been effectively applied to account for the electrical properties of a wide range of transition metal oxide glasses^[5-6,19]. For polaron to be a small, the polaron radius should be greater than the radius of the ion on which the electron is localized but less than the distance R separating two sites^[8]. As it is evident for the present glass systems (Table 6.11), the value of polaron radius 1.675 Å to 1.822 Å for 1st series, 1.975 Å to 1.583 Å for 2nd and 1.583 Å to 1.975 Å in 3rd series which are less than the R [4.16 Å to 4.52 Å, 3.93 Å to 4.90 Å and 4.31 Å to 4.52 Å in 1st, 2nd and 3rd series respectively], which satisfies the condition for small polaron hopping. A similar types of results were also reported for $\text{SiO}_2\text{-V}_2\text{O}_5\text{-P}_2\text{O}_5$ ^[9] and $\text{PbO-P}_2\text{O}_5\text{-V}_2\text{O}_5$ glasses^[10]. It has also been established from the Seebeck coefficient measurement (Section 6.3) that the value of α' (a constant of proportionality between the heat of transfer and the kinetic energy of electron), is much less than the unity i.e., $\alpha' \ll 1$ ^[11,20], which lies in the range of 0.011 to 0.0848 for these glasses and supports the conduction for small polaron hopping. H. Mori^[17] reported a similar kind of results.

6.14 ADIABATIC CONDUCTIVITY:

Linsley et. al.^[13], Graves et. al.^[21] and Sayer et.al.^[6] have suggested that the V₂O₅-P₂O₅ and WO₃-P₂O₅^[15] glasses follow the adiabatic approximation while V₂O₅-TeO₂^[22], FeO-P₂O₅^[23-24] etc., glasses exhibit non-adiabatic character. Adiabatic hopping has been observed for PbO-SiO₂-Fe₂O₃ glass system by Anderson R. A. and Mac Crone R. K.^[22].

The conductivity of the transition metal oxide glasses is given by Equation 6.12 where the pre-exponential term σ_0 can be given as

$$\sigma_0 = \frac{\nu_0 e^2 c(1-c)}{kTR} \exp(-2\alpha R) \quad (6.13)$$

The value of c were estimated from the photometric titration analysis (Chapter 3.6). The value of α , the electron wave function decay constant, were estimated by knowing the values of c , R and σ_0 ^[22]. The calculated values of α from Equation 6.13 lie in the range from 4.99 Å to 4.39 Å, 5.28 Å to 4.05 Å and 4.67 Å to 4.39 Å for the samples of first, second and third series respectively and αR have been calculated which are observed to be constant for all the sample compositions. These values of α are also consistent with those obtained by Hirashima and Yoshida^[25].

Sayer and Mansingh^[6] noted that a plot of $\log \sigma$ versus activation energy W at a certain temperature allows one to distinguish between adiabatic and non-adiabatic hopping and judge the relative importance of the two exponential terms. The calculated temperature, T_c , estimated from the slope $(1/2.303T_c)$ of such a plot will be close to T if $\exp(-2\alpha R)$ term in Equation 6.12 does not contribute to the conductivity and will be different from T if Equation 6.11 is more appropriate, i.e., $\exp(-2\alpha R)$ term contributes to the conductivity. In this case, αR changes with composition^[4]. Figures 6.12 (a), (b) & (c) show the plots of $\log \sigma$ versus W at three different temperatures. The

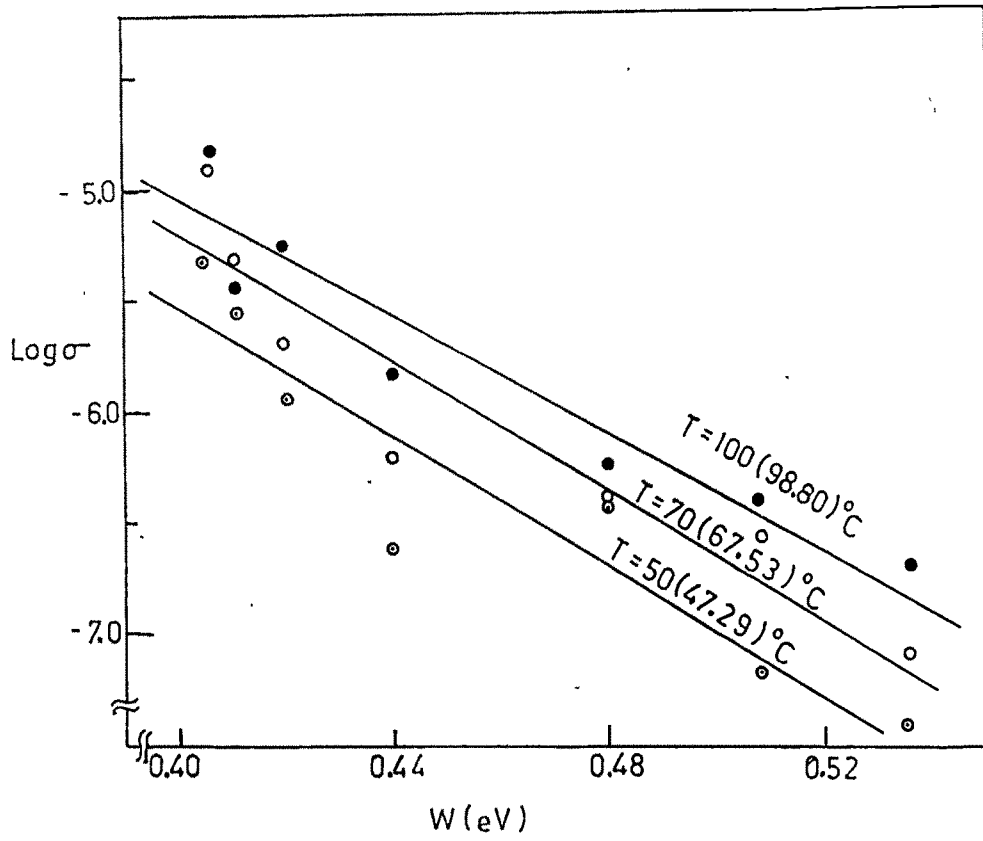


Figure 6.12 (a) : Plot of $\text{Log } \sigma$ versus W (eV) for series 1.

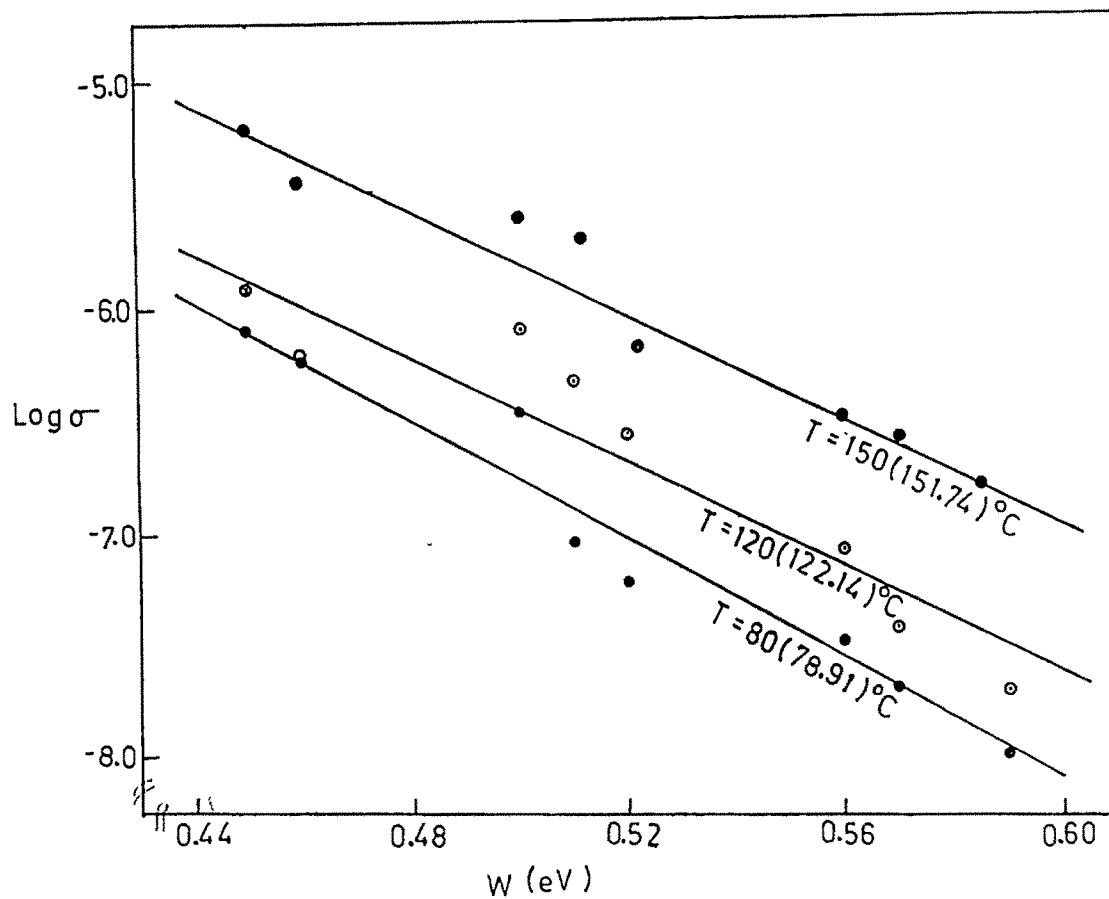


Figure 6.12 (b) : Plot of $\text{Log } \sigma$ versus W (eV) for series 2.

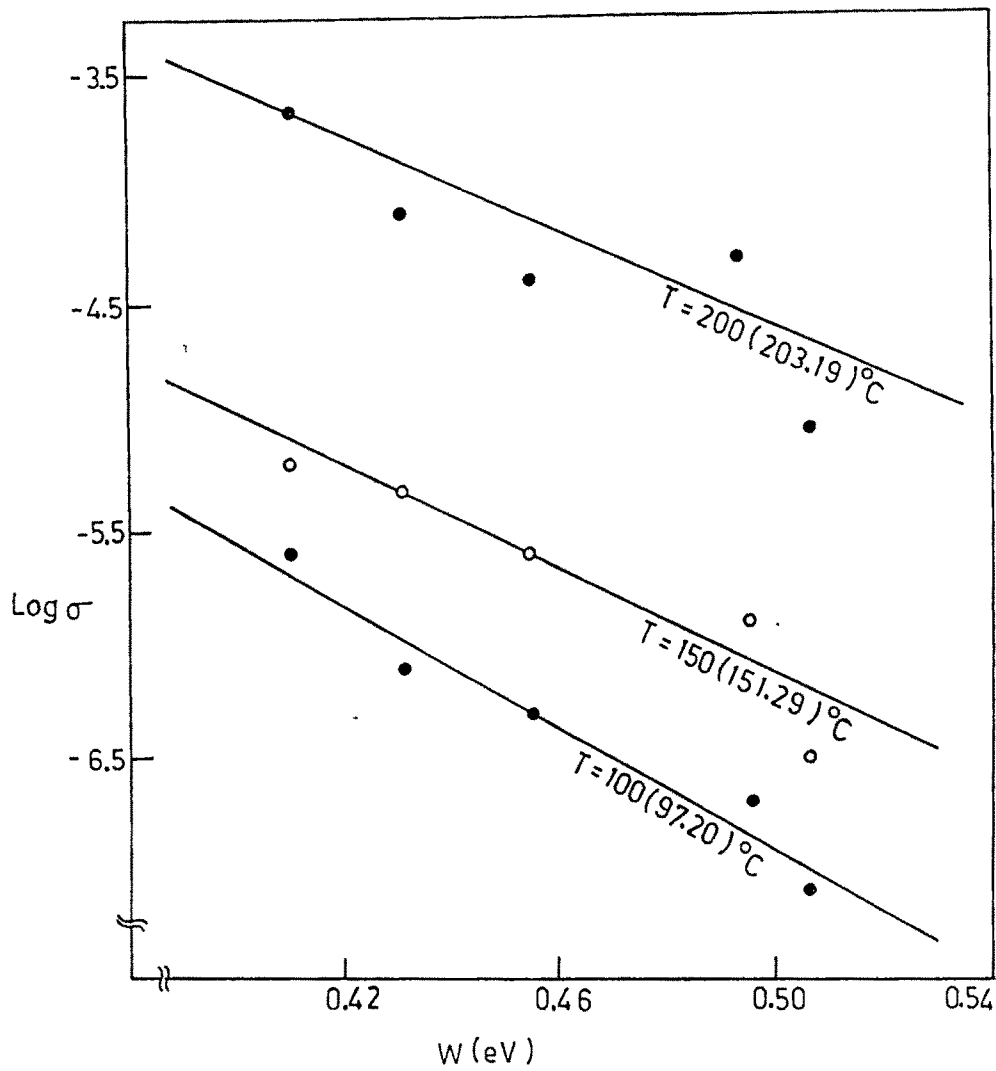


Figure 6.12 (c) : Plot of $\text{Log } \sigma$ versus $W(\text{eV})$ for series 3.

temperature T_C estimated from the slope of each line for all the glass series are close to T and αR term remains almost constant irrespective of composition, means hopping can be ascribed as adiabatic and the tunneling term α in Equation 6.12 does not contribute to the conductivity. Murawski et. al.^[2] and Sayer et.al.^[6] suggested that in Equation 1, the contribution of α term in the conductivity can be also checked by plotting $\log\sigma$ versus W at a fixed temperature. They also reported the adiabatic hopping in the V_2O_5 based glasses.

Holstein^[26] suggested that the hopping process is controlled by the activation energy and is given by the following equations

$$J > \left[\frac{2kTW_H}{\pi} \right]^{1/4} \left[\frac{h\nu_o}{\pi} \right]^{1/2} \quad (\text{adiabatic hopping}) \quad (6.14)$$

and

$$J < \left[\frac{2kTW_H}{\pi} \right]^{1/4} \left[\frac{h\nu_o}{\pi} \right]^{1/2} \quad (\text{non-adiabatic hopping})$$

The value J , the integral overlap function [$J \approx \exp(-2\alpha R)$] were estimated by^[27] $J = W_{H(\text{mean})} - W$. Dhawan et. al.^[8] reported the value of $J \sim 0.01$ eV, which satisfies the criterion for small polaron formation but not for adiabatic hopping if ν_o is taken as 10^{13} Hz and also discussed that if calculated by taking 10^{11} Hz in Equation 6.11, then the right hand side of Equation 6.14 will become 0.003 eV and condition for adiabatic hopping is satisfied. The values of W_H is calculated by using^[28]

$$W_H = \frac{e^2}{4\epsilon_p} \left[\frac{1}{v_p} - \frac{1}{R} \right] \quad (6.15)$$

Where v_p is polaron radius and R is the average spacing between vanadium ions. The value of v_p is calculated by^[4,28]

$$v_p = \frac{1}{2} \left(\frac{\pi}{6N} \right)^{1/3} \quad (6.16)$$

Where, N is the site density calculated from density measurements (Chapter 4.4). The average site spacing, R , between vanadium ions is also calculated from density measurements. The value of polaron radius, r_p , lie in the range of 1.58 °A to 1.98 °A and R for all the glass samples lie in the range of ≈ 3.93 °A to 4.90 °A, which is greater than the estimated value of R (3.60 °A) for V_2O_5 ^[5-7]. The calculated values of W_H lie in the range of 0.312 eV to 0.347 eV (Table 6.11).

The value of right hand side of the Equation 6.14 were calculated for an optical phonon frequency of $\approx 10^{13}$ Hz. These values lie in the range of 0.0123 to 0.0128 eV. These values are less than the value of J which lie between 0.0689-0.255 eV (Table 6.11), satisfying the condition for adiabatic hopping. Hirashima et. al.^[10] also reported the adiabatic hopping in $PbO-P_2O_5-V_2O_5$ glasses by assuming the value of $h\nu_o$ equals to 29kJ/mole.

Hence, it can be ascribed that all the glass samples in present glass systems exhibit a semiconducting adiabatic hopping due to small polarons.

6.15 EFFECT OF GLASS MODIFIER K_2O ON $xK_2O:(95-x)$ $[2V_2O_5:B_2O_3]: 5Fe_2O_3$:

Glass modifier plays a very important role for the formation of glasses and also has characteristics to change the properties of glasses like electrical conductivity, switching etc. The dependence of the glass modifier on the conductivity in the glasses has also been studied by many workers [10, 29-30]. In the present glass system, the amount of glass modifier increases from 0 to 30 mole % whereas, the amount of V_2O_5 is decreasing with the simultaneous decrease of B_2O_3 . The amount of Fe_2O_3 has been kept constant in all the glass samples as 5 mole %. Figure 6.13 (a) shows the dependence of the conductivity on the amount of the modifier. As the amount of glass modifier, K_2O , is introduced to the glass structure, it is supposed to go into network at interstitial position. In the present glass system, B_2O_3 and V_2O_5 are taken as glass formers, therefore, it may be assumed that K_2O by going into B_2O_3 and V_2O_5 network modify and break their structures. Because of the breaking of V_2O_5 structure, the atomic site spacing between V-V increases. The V-V spacing calculated from the density measurements is observed to change from 4.16 Å to 4.52 Å which may not only inhibit the mobility of small polarons but also require more energy to hop from one site to another resulting into decrease of conductivity from 1.59×10^{-5} to $2.04 \times 10^{-7} \Omega^{-1}cm^{-1}$ (at 100°C) and increase of activation energy from 0.407 eV to 0.536 eV. Sanches et. al. [31] also discussed that the decrease of the conductivity arises from a decrease in the mobility of the charge carriers as a result of increase of V-V spacing. Thus with the increase of K_2O amount, the atomic site spacing between V-V is found to increase which directly affects the mobility of a charge carrier. Also the value of $c (V^{+4}/V_{total})$ is also observed to be dependent on K_2O amount (Table 6.12). Figure 6.14 (a) shows the plot of log of conductivity σ (at 100 °C) and activation energy, W , versus V-V spacing. It is found that the

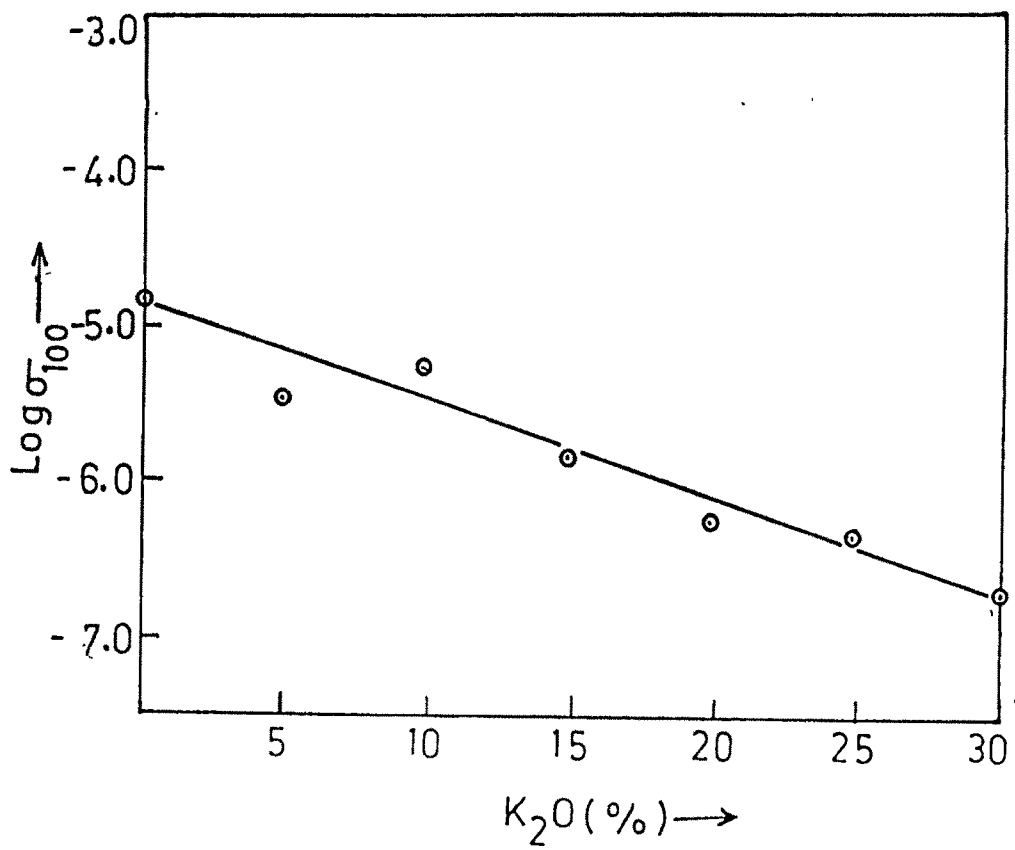


Figure 6.13 (a) : Plot of $\text{Log } \sigma_{100}$ versus K_2O mole % for series 1.

Table 6.12 : Electrical Conductivity data of Series 1, 2 and 3.

Series	K ₂ O Mole %	W (eV)	W _H (eV)	W _D (eV)	v _p (Å)	V ²⁺ 10 ²⁰	V ³⁺ /	V-V spacing (Å)	Fe-Fe spacing (Å)	σ ₁₀₀ Ω ⁻¹ Cm ⁻¹	μ mobility cm ² V ⁻¹ S ⁻¹
Series 1	0	0.407	0.327	0.161	1.67	2.14	0.0154	4.16	11.33	1.59 x 10 ⁻⁵	4.70 x 10 ⁻⁷
	5	0.411	0.332	0.158	1.68	2.96	0.0216	4.18	11.18	3.55 x 10 ⁻⁶	7.50 x 10 ⁻⁸
	10	0.420	0.336	0.168	1.70	3.19	0.0239	4.22	11.08	5.62 x 10 ⁻⁶	1.11 x 10 ⁻⁷
	15	0.442	0.339	0.205	1.72	3.24	0.0256	4.27	11.00	1.59 x 10 ⁻⁶	3.10 x 10 ⁻⁸
	20	0.479	0.342	0.273	1.74	3.91	0.0317	4.33	10.91	5.62 x 10 ⁻⁷	9.00 x 10 ⁻⁹
	25	0.509	0.347	0.324	1.76	3.98	0.0332	4.37	10.76	4.47 x 10 ⁻⁷	7.00 x 10 ⁻⁹
	30	0.536	0.343	0.386	1.82	4.16	0.0385	4.52	10.86	2.04 x 10 ⁻⁷	3.10 x 10 ⁻⁹
Series 2	V ₂ O ₅ =40 %	0.585	0.327	0.516	1.975	8.17	0.096	4.90	11.47	1.78 x 10 ⁻⁸	1.36x 10 ⁻¹¹
	45	0.572	0.337	0.469	1.843	7.90	0.0756	4.57	11.13	2.51 x 10 ⁻⁸	1.99 x 10 ⁻¹⁰
	50	0.556	0.340	0.431	1.756	6.88	0.0570	4.36	10.98	3.39 x 10 ⁻⁸	3.07 x 10 ⁻¹⁰
	55	0.522	0.336	0.372	1.716	5.36	0.0414	4.26	11.07	1.29 x 10 ⁻⁷	1.50 x 10 ⁻⁹
	60	0.512	0.333	0.358	1.665	4.67	0.0329	4.13	11.06	2.40 x 10 ⁻⁷	3.21 x 10 ⁻⁹
	65	0.501	0.327	0.349	1.635	3.56	0.0238	4.06	11.16	4.47 x 10 ⁻⁷	7.84 x 10 ⁻⁹
	70	0.459	0.321	0.277	1.609	3.39	0.0216	3.99	11.25	6.31 x 10 ⁻⁷	1.16 x 10 ⁻⁸
75	0.451	0.315	0.273	1.583	2.59	0.0157	3.93	11.33	1.00 x 10 ⁻⁶	2.41 x 10 ⁻⁸	
Series 3	Fe ₂ O ₃ =5 %	0.410	0.343	0.135	1.738	2.58	0.0207	4.31	10.99	2.40 x 10 ⁻⁶	5.82 x 10 ⁻⁸
	7.5	0.431	0.334	0.195	1.746	2.79	0.0226	4.33	9.06	8.59 x 10 ⁻⁷	1.92 x 10 ⁻⁸
	10	0.455	0.327	0.256	1.760	3.03	0.0252	4.37	8.69	5.13 x 10 ⁻⁷	1.06 x 10 ⁻⁸
	12.5	0.496	0.319	0.354	1.788	3.20	0.0279	4.44	8.05	2.00 x 10 ⁻⁷	3.89 x 10 ⁻⁸
	15	0.506	0.313	0.387	1.820	3.40	0.0313	4.52	7.52	7.94 x 10 ⁻⁸	1.46 x 10 ⁻⁹

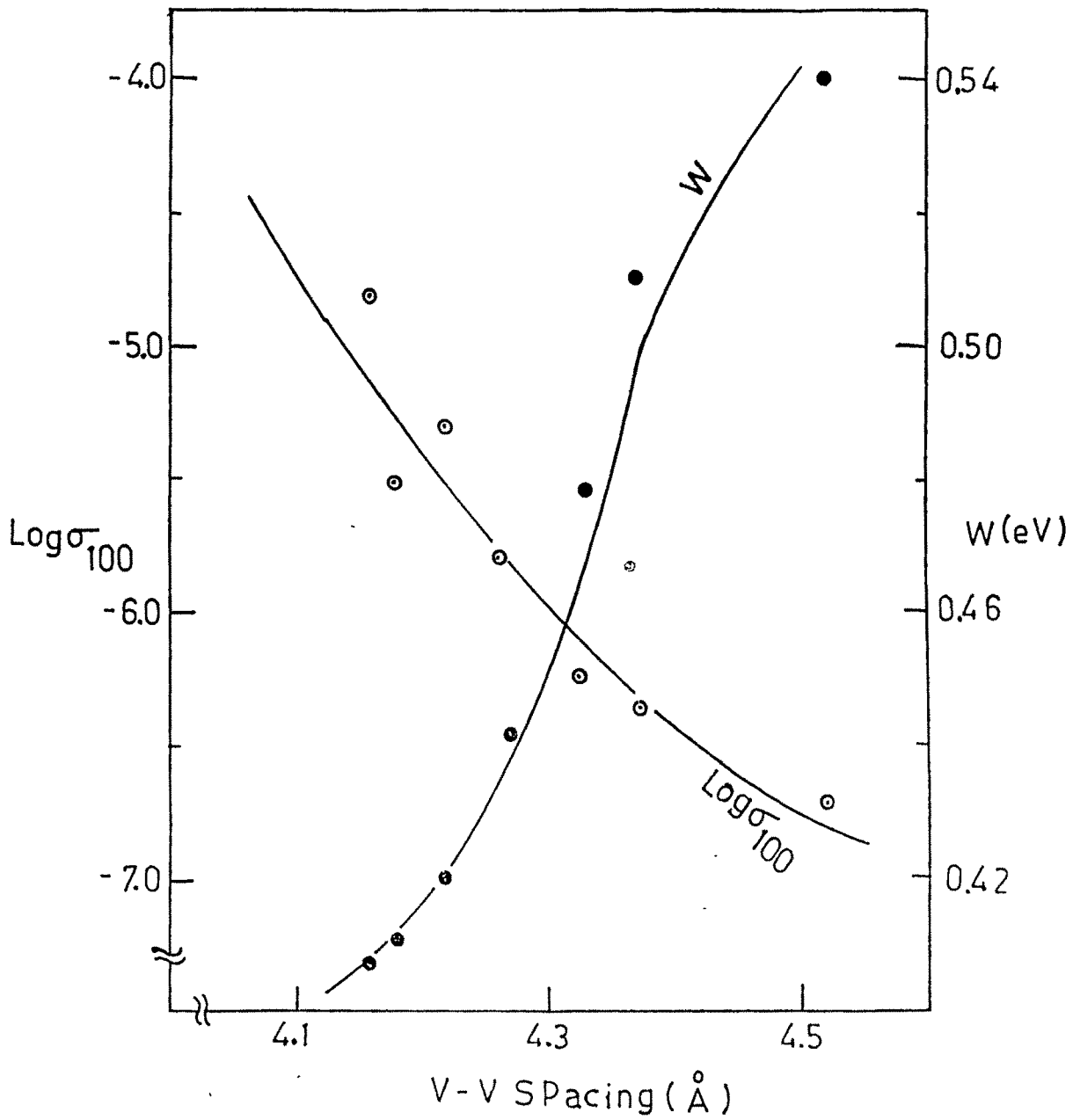


Figure 6.14(a) : Plot of $\text{Log}\sigma_{100}$ and $W(\text{eV})$ versus V-V spacing for series 1.

conductivity decreases whereas the activation energy increases with increase of V-V spacing. Figure 6.15 represent the variation of activation energy with modifier K_2O . The observed activation energy were found to be slightly higher than the values obtained for other V_2O_5 based glasses [6-8,11]. This may be due to the presence of B_2O_3 glass former in these glasses, which does not take part in this conduction process. It is also observed from Table 6.12 that the decrease in conductivity (at 100 °C), in the samples containing K_2O less than 20 mole % is 84 % whereas, decrease in the conductivity is observed by 63.7 % for those which contain K_2O greater than 20 mole %. The calculated V-V spacing, R , for K_2O less than 20 mole % increases by 3.6 % whereas, for K_2O greater than 20 mole % V-V spacing increases by 4.4 % Thus a greater change in the conductivity can be expected for K_2O greater than 20 mole % because of the larger change in V-V spacing as compared to K_2O less than 20 mole %. But, small change in the conductivity is observed for K_2O greater than 20 mole %. This may be due to the fact that the Fe_2O_3 may also take part in the conduction process by the following possible transition between $Fe^{+2}-Fe^{+3}$, $Fe^{+3}-V^{+4}$ and $Fe^{+2}-V^{+5}$ [32-33]. However, the presence of Fe^{+2} ions has not been observed by Mössbauer spectra and /or by chemical analysis [20,34]. Therefore, the possibility of transition between $Fe^{+2}-Fe^{+3}$ or $Fe^{+2}-V^{+5}$ is ruled out. Only transition between $Fe^{+3}-V^{+4}$ may be considered which may help in enhancing the conductivity of these glasses. It has been also discussed for $ZnO-B_2O_3-Fe_2O_3-V_2O_5$ [35] glasses that the interaction of V^{+4} and Fe^{+3} ions lead to the formation of $V^{+4}-O-Fe^{+3}$ groups and in such case the polaron has higher mobility and offers a higher conductivity and low activation energy. In the present glass system Fe-Fe spacing is decreasing and V-V spacing is increasing (Table 6.12). Thus effective spacing between Fe^{+3} and V^{+4} ions is increased which requires a larger hopping energy for conduction. The calculated hopping energy increase from 0.32 eV to 0.34 eV, disorder energy 0.161 eV to 0.368 eV and

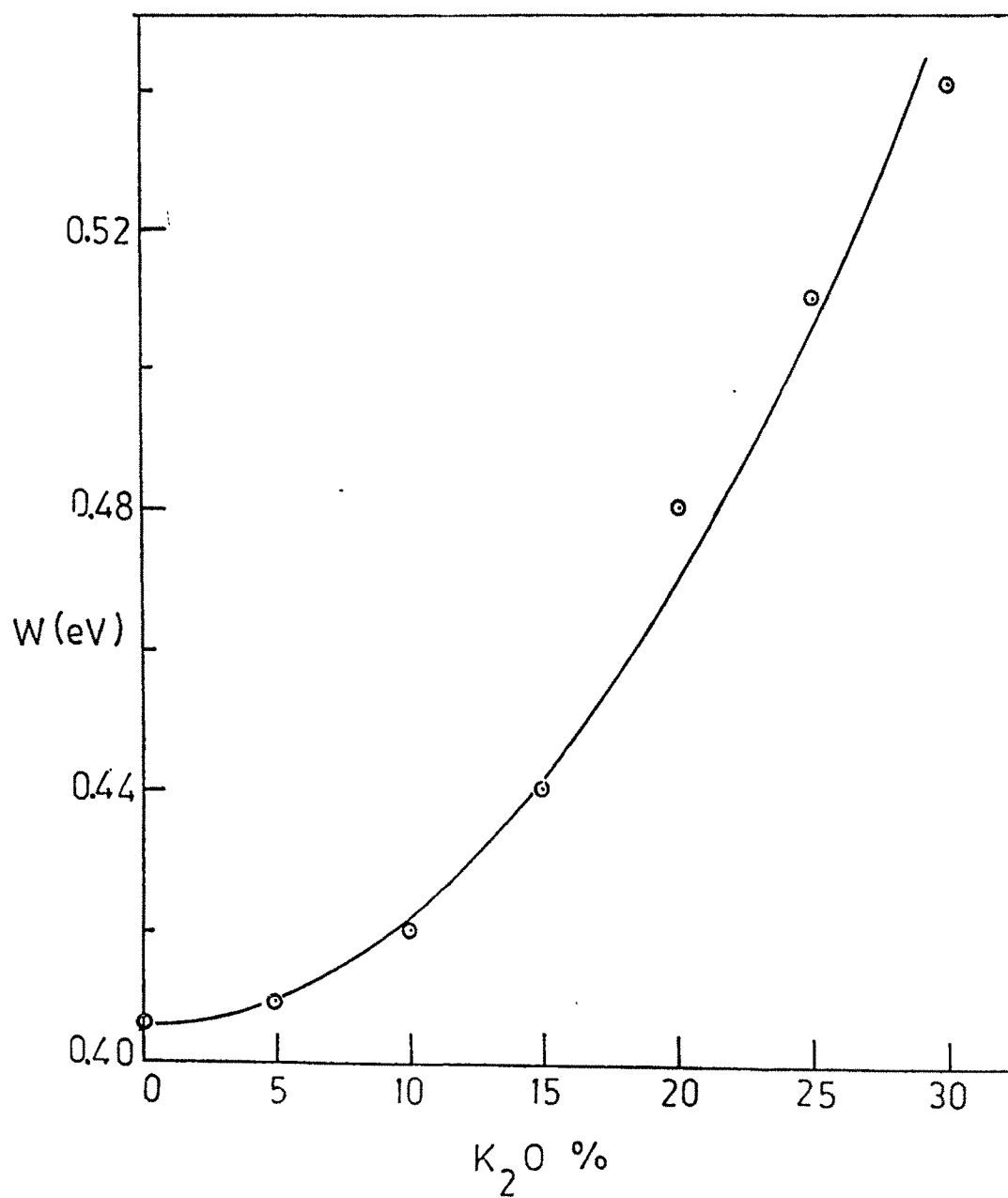


Figure 6.15 : Plot of W(eV) versus K₂O mole % for series 1.

consequently the mobility of charge carriers decreases from 4.6×10^{-7} to $9 \times 10^{-9} \text{ cm}^2\text{V}^{-1}\text{s}^{-1}$. Thus, the conductivity expected to decrease. A similar kind of results were also reported in phosphate and borate glasses containing two transition metal oxides^[36-37].

Hence, the resulting effect of the present composition is to decrease the conductivity and increase of the activation energy with the increasing amount of glass modifier.

6.16 EFFECT OF GLASS FORMERS ON 20K₂O: yV₂O₅: (75-y) :B₂O₃: 5Fe₂O₃ GLASS SYSTEM.

Electrical conductivity of 20K₂O: yV₂O₅: (75-y)B₂O₃: 5Fe₂O₃ glass system has been studied in which the effect of glass former V₂O₅ on the conductivity has been attempted to study. Many authors studied the effect of glass former V₂O₅ on the electrical conductivity, where the increase of the conductivity has been reported with the increase of V₂O₅ contents^[4,9-10,30,37]. As V₂O₅ is a conditional glass former^[11], it does not make glass easily even in presence of the glass modifier. Electrical conductivity of these glasses has been studied by keeping glass modifier K₂O and Fe₂O₃ as constant in this series.

Figure 6.13(b) shows the plot of Log σ at 100°C (conductivity) versus V₂O₅ amount, which shows the increase of the conductivity with increasing V₂O₅ amount. Figure 6.14(b) shows the plot of Log σ_{100} and activation energy, W, versus V-V spacing. The increase of the conductivity and decrease of activation energy with decreasing V-V spacing, R has been observed. Ghosh et. al.,^[4] and Dhawan et. al.,^[8] also reported the activation energy and the conductivity with the variation of V-V spacing. In the present study the conductivity of glass samples at 100 °C lie in the range 1.78×10^{-8} to $1.00 \times 10^{-6} \Omega^{-1}\text{Cm}^{-1}$, the activation energy from 0.585 eV to 0.451 eV and V-V spacing, R, from 4.90 Å to 3.93 Å. The following possible reasons may be assigned for the increase of the conductivity and decrease of the activation energy in this series.

(a) The amount of K₂O has been kept constant i.e., 20 mole %. By increasing y, the number of K⁺ ions interacting with V₂O₅ structure decrease due to K₂O:V₂O₅ ratio which decrease the V-V spacing in these glasses.

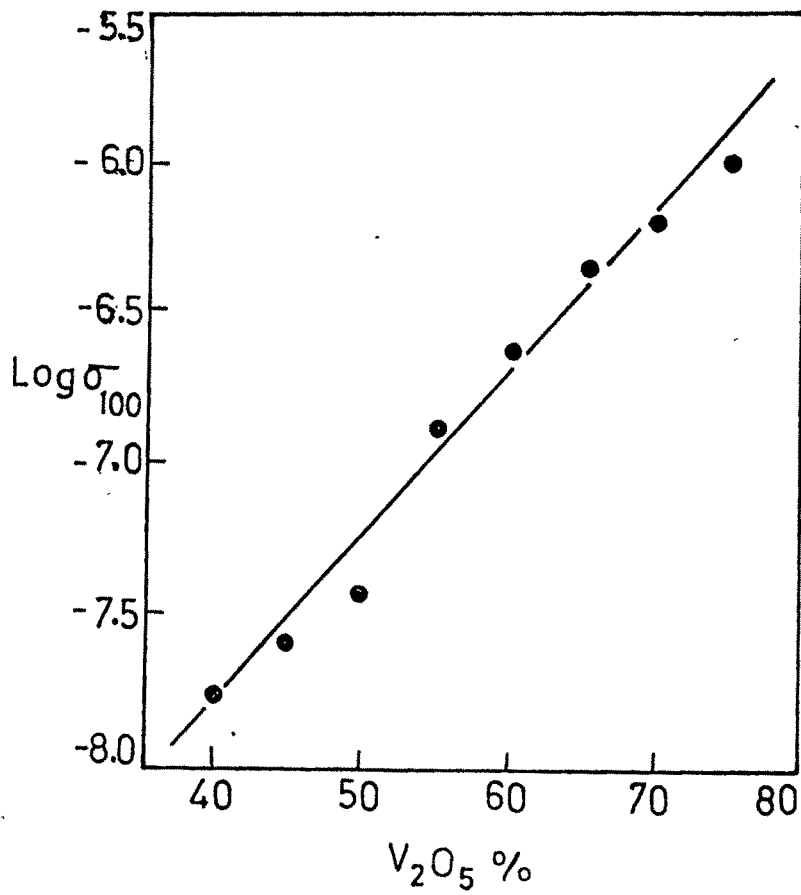


Figure 6.13 (b) : Plot of $\text{Log } \sigma_{100}$ versus V_2O_5 mole % for series 2.

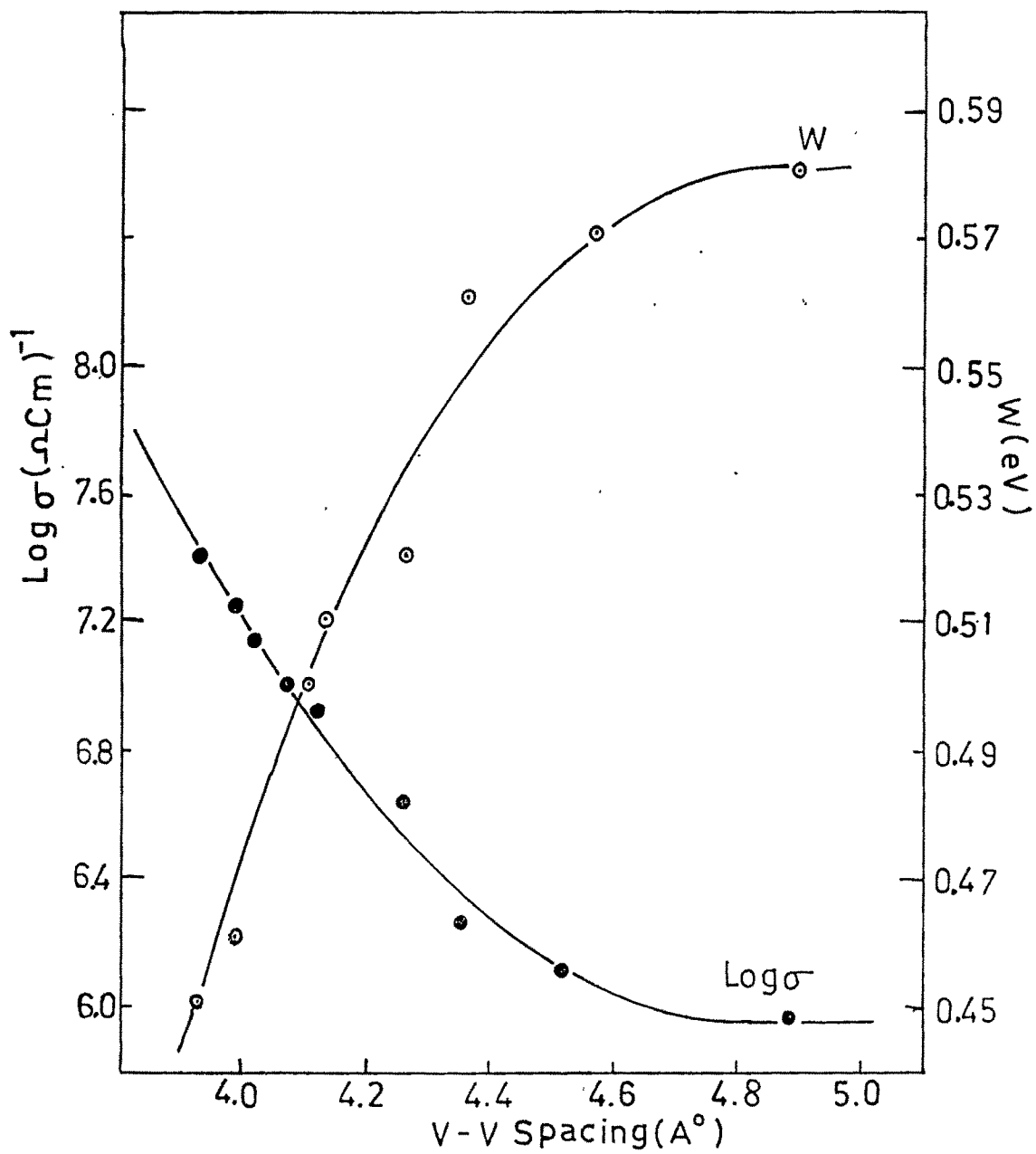


Figure 6.14(b): Plot of $\text{Log} \sigma_{100}$ and $W(\text{eV})$ versus V-V spacing for series 2.

(b) The density of the present glass system is increased from 2.184 gm/cc to 2.979 gm/cc (Chapter 4.4) indicating a closely packing of the glass structure as a result of decrease of the distance between atoms (i.e. Vanadium atoms) which may be responsible for decreasing the V-V spacing. Also, the increase in the mobility of a charge carrier from $1.36 \times 10^{-11} \text{ cm}^2\text{V}^{-1}\text{s}^{-1}$ to $2.41 \times 10^{-8} \text{ cm}^2\text{V}^{-1}\text{s}^{-1}$ has been observed which requires less energy to hop and the disorder energy observed to be decreased from 0.515 eV to 0.273 eV (Table 6.12). As a result of which the conductivity of the present glass system increases.

(c) Chemical analysis shows that a decrease in the concentration of lower valence state (V^{+4} ions) rapidly increases the conductivity (Table 6.12)^[33]. The ratio $\ln\text{V}^{+5}/\text{V}^{+4}$ indicate that the conductivity increases with increasing V^{+5} state of vanadium in glass. The calculated activation energy is also found to be dependent on $\text{V}^{+5}/\text{V}^{+4}$ ratio^[11,33]. The Figure 6.16 shows the dependence of the activation energy on $\ln\text{V}^{+5}/\text{V}^{+4}$ ratio. It is observed that

- (i) Activation energy, W , is directly related to $\ln\text{V}^{+5}/\text{V}^{+4}$ (Figure 6.16).
- (ii) Activation energy, E , decreases as the concentration of V_2O_5 increases as a result of rapid increase of $\ln \text{V}^{+5}/\text{V}^{+4}$. Thus, the decrease of the activation energy with increase of $\ln \text{V}^{+5}/\text{V}^{+4}$ leads to increase the conductivity in these type of glasses.

The dependence of the activation energy, W , on $\text{V}^{+5}/\text{V}^{+4}$ ratio was also observed in $\text{GeO}_2\text{-P}_4\text{O}_{10}\text{-V}_2\text{O}_5$ ^[33] and $\text{V}_2\text{O}_5\text{-BaO-K}_2\text{O-ZnO}$ ^[11] systems.

(d) As the amount of Fe_2O_3 in the present glass series has been kept constant which also takes part in the conduction process through $\text{Fe}^{+3}\text{-V}^{+4}$ transition^[32-33,38-41] (Section 6.13). Calculated values of Fe-Fe spacing (from density measurement) remains almost constant i.e. 11.30 Å. As it is evident that V-V spacing decreases (Table 6.12) from 4.90 Å to 3.93 Å whereas, Fe-Fe spacing remains constant, therefore, an increase in spatial distance between Fe^{+3} and V^{+4} ions can be expected which decreases the conduction between Fe^{+3} and V^{+4} ions.

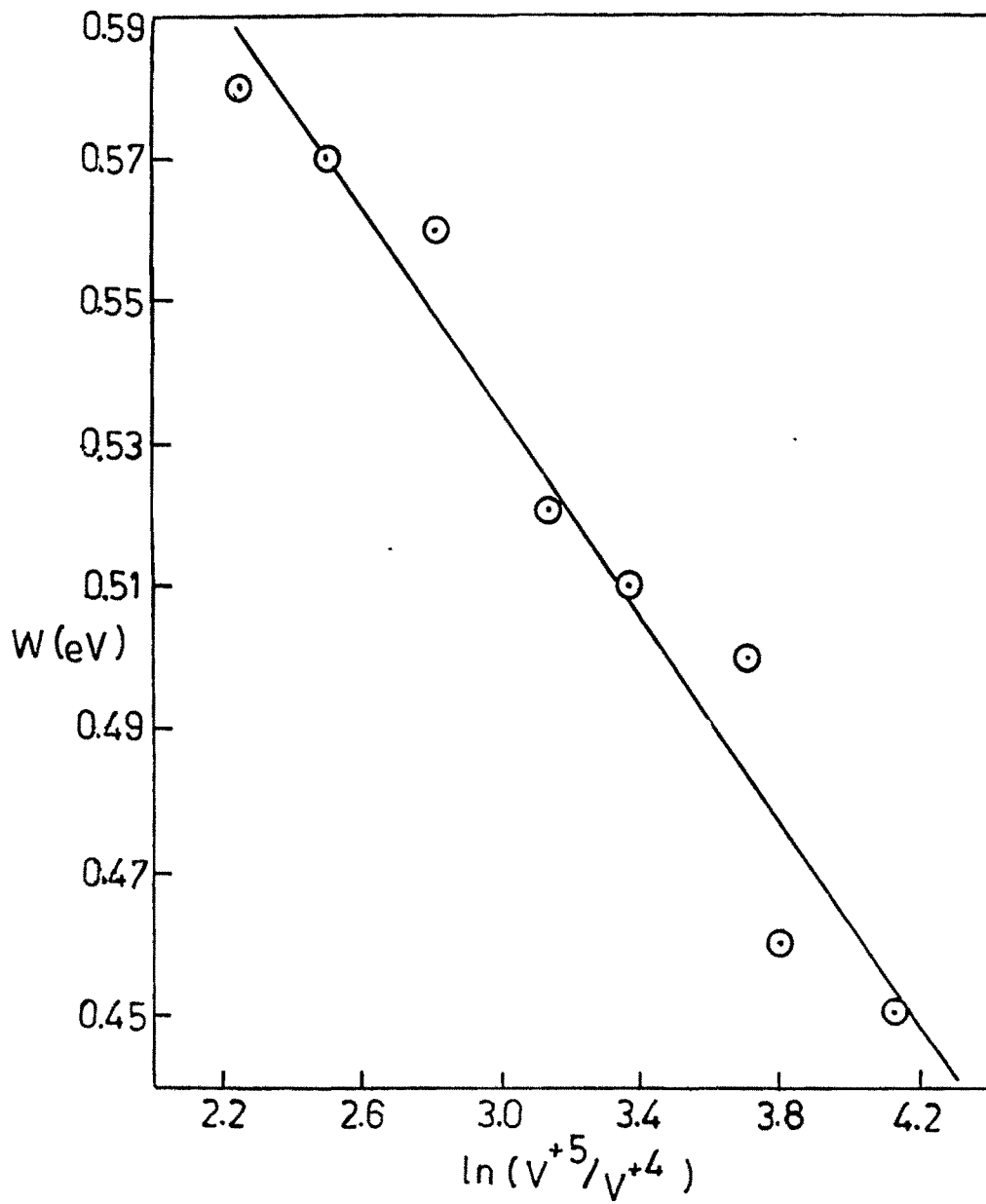


Figure 6.16 : Plot of W(eV) versus $\ln(V^{+5}/V^{+4})$ for series 2.

But in the present glass system increase in the conductivity with y is observed. Hence, in the present glass system, effect of V_2O_5 on the conductivity can be expected due to $V^{+5}-V^{+4}$ transition which masks the decrease of conductivity due to increase in distance between Fe^{+3} and V^{+4} ions.

Thus it can be ascribed that

- (i) Due to decrease of V-V spacing, R , in the glass, the hopping process between V^{+4} and V^{+5} is to increase the conductivity which dominates the effect of decrease in conductivity due to increase in $Fe^{+3}-V^{+4}$ distance.
- (ii) It is the glass former V_2O_5 which is responsible for semiconducting nature and the increase of conductivity in this series..

6.17 Effect of Fe_2O_3 ON $xK_2O:(100-x-y)[(1+n)V_2O_5: B_2O_3]:yFe_2O_3$ GLASSES.

The dependence of conductivity on Fe_2O_3 amount were discussed by many workers [30,32-33,40,42]. The electrical transport properties on the glass system $(Fe_2O_3)_x(V_2O_5)_{1-x}$ was investigated where the sample exhibited a thermally activated hopping conduction^[40]. The electrical conduction mechanism of the system $Fe_2O_3-V_2O_5$ was reported by Kurina L. N. and Ediseeva O. N.^[43] and Burzo E.^[44]. They also discussed that the introduction of Fe_2O_3 causes a decrease in conductivity. In the present glass system, attempt has been made to study the effect of Fe_2O_3 on conductivity and activation energy.

Figure 6.13 (c) shows the decrease of the conductivity with Fe_2O_3 amount. The increase of Fe_2O_3 amount in the glasses leads to the formation of $Fe^{+3}-Fe^{+3}$ associates which coexists with $V^{+4}-Fe^{+3}$ associates^[41]. All investigators of glasses containing both Fe_2O_3 and V_2O_5 pointed out the formation of mixed clusters of V^{+4} and Fe^{+3} ions and discussed their effect on the electrical conductivity of glasses^[39-41]. In the present glass system, an

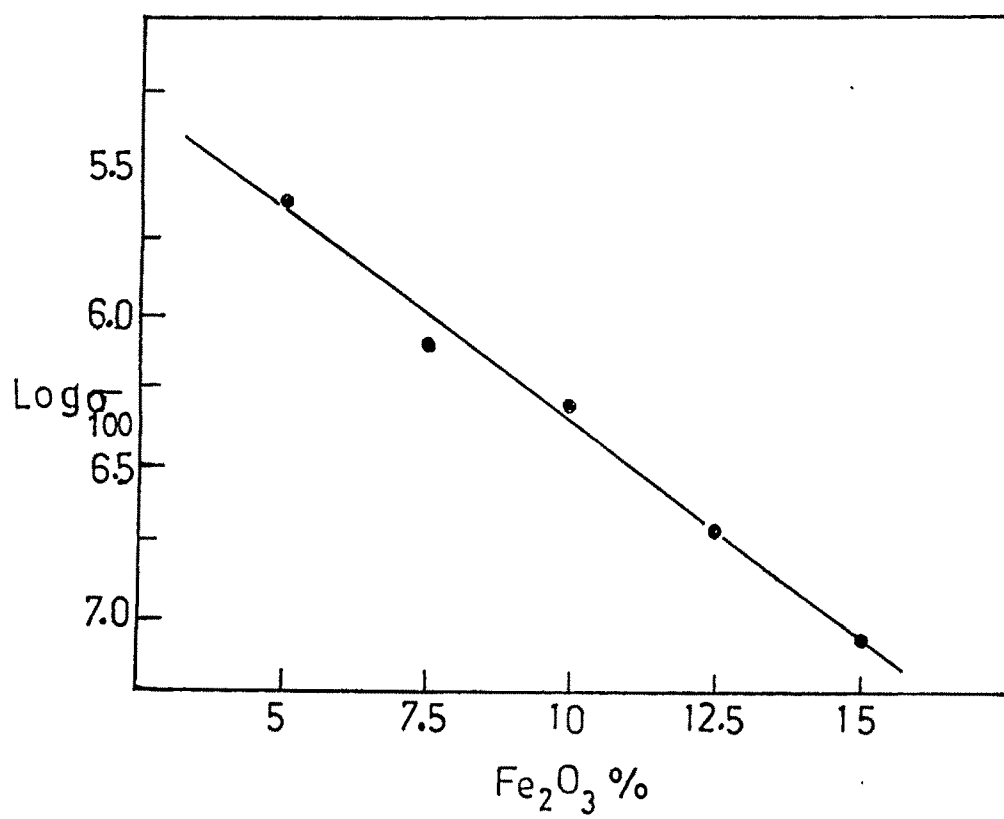


Figure 6.13 (c) : Plot of $\text{Log}\sigma_{100}$ versus Fe_2O_3 mole % for series 3.

increase of K_2O also affects the V-V spacing which increases from 4.31 \AA to 4.52 \AA [Section 6.13]. An increase of Fe_2O_3 amount leads to decrease the Fe-Fe spacing from 10.997 \AA to 7.523 \AA . It has also been discussed that an incorporation of Fe^{+3} ions into the vanadate skeleton leads to increase of average spacing between vanadium sites with Fe_2O_3 concentration^[41]. The effect of the addition of Fe_2O_3 in glasses on activation energy and conductivity can also be presumably explained by change in distance between vanadium sites^[34,41]. An average spacing between Fe^{+3} and V^{+4} ions increases, which requires a larger energy for hopping and the mobility of the charge carriers found to decrease from $5.82 \times 10^{-8} \text{ cm}^2 \text{v}^{-1} \text{s}^{-1}$ to $1.46 \times 10^{-9} \text{ cm}^2 \text{v}^{-1} \text{s}^{-1}$, which decreases the conductivity of glass system, which lie in the range of 2.40×10^{-6} to $7.94 \times 10^{-8} \text{ } \Omega^{-1} \text{ cm}^{-1}$ (Table 6.12). Figure 6.14(c) shows a plot of log of conductivity at $100 \text{ }^\circ\text{C}$ and activation energy W , versus V-V spacing. It has been observed that the conductivity at $100 \text{ }^\circ\text{C}$ decreases and the activation energy increases with V-V spacing. An increase in the activation energy and decrease of conductivity with the decrease of V_2O_5 amount has been interpreted^[30] in terms of increase of the distance R , between vanadium sites. It has been also discussed in section 6.13 that an increase of K_2O in the glasses also affects the spacing in vanadium site and thereby decreases the conductivity of glasses. Thus, to get a clear picture of about an effect of Fe_2O_3 in the glasses, one sample has been prepared with zero amount of Fe_2O_3 using $5K_2O:95[1.2V_2O_5: B_2O_3]$. The conductivity of glasses for zero amount of Fe_2O_3 is $1.89 \times 10^{-7} \text{ } \Omega^{-1} \text{ cm}^{-1}$ which increases by 92% for 5% of Fe_2O_3 but no amount of K_2O in the glasses.. Thus incorporation of Fe_2O_3 in the glasses increases the conductivity. In the second sample of 3rd glass series which contains 5 mole % of K_2O and 7.5 mole % Fe_2O_3 , if the conductivities of these two samples are compared, it is clear that the conductivity is larger for the glass sample with 7.5 mole % of Fe_2O_3 than that with zero amount of Fe_2O_3 . It means Fe^{+3} ions participate in conduction process in the present glass systems.

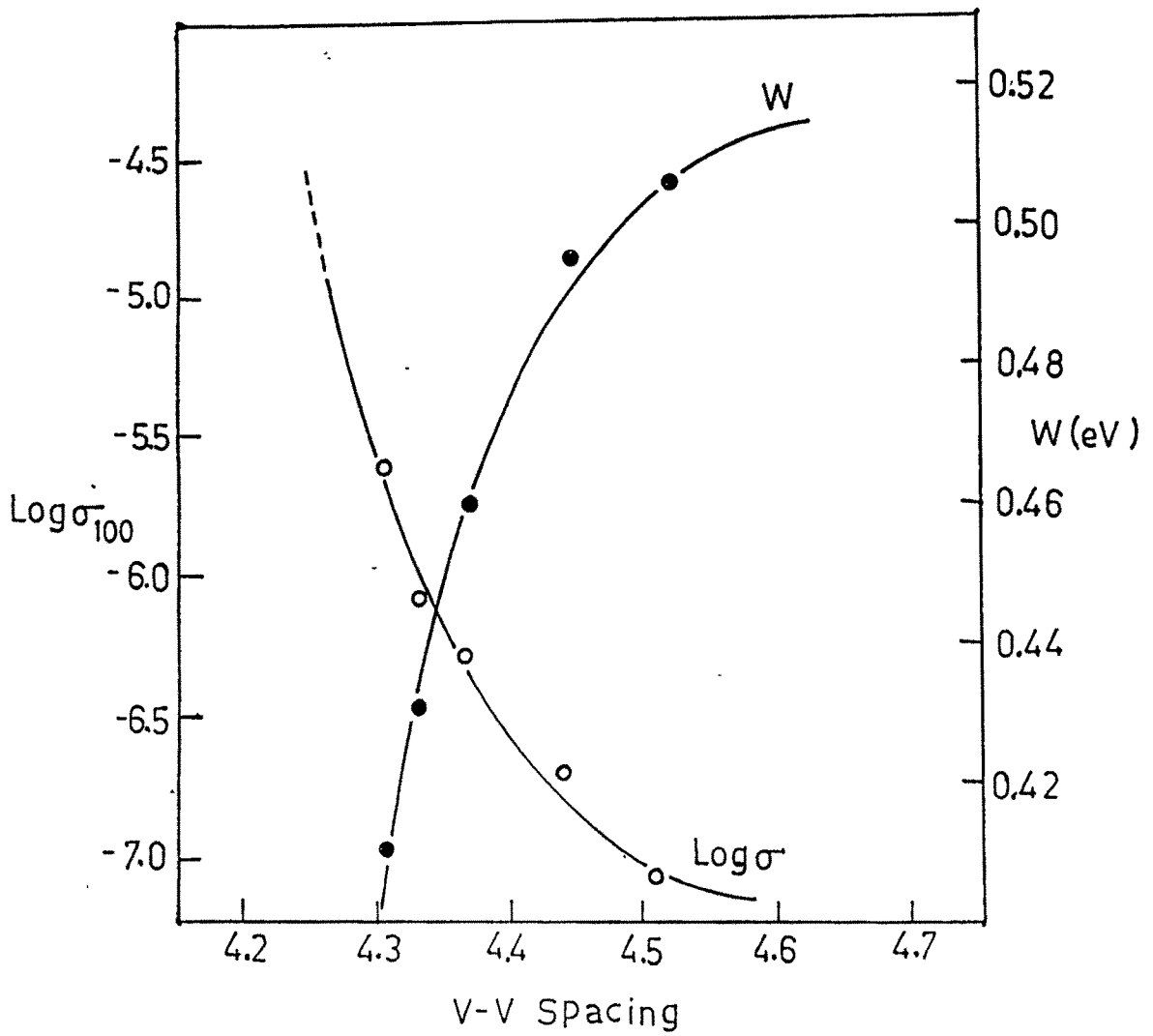


Figure 6.14 (c) : Plot of $\text{Log}\sigma_{100}$ and $W(\text{eV})$ versus V-V spacing for series 3.

However, the decrease in Fe-Fe spacing should be responsible for increasing the conductivity, but at the same time, V-V spacing increases in the glass samples which produces the reverse effect. Therefore, the average effect, which has been observed, is to decrease the conductivity. This may be due to the fact that

- (i) an increase between Fe^{+3} and V^{+4} spacing and V^{+4} and V^{+5} , decreases the conductivity.
- (ii) due to the non-existence of Fe^{+2} ions in all the samples, conduction between Fe^{+2} and Fe^{+3} does not exist.

Reference :

1. Abhai Mansingh, J. K. Vaid, R. P. Tandon, *J. of Phy., Solid State Phy.*, Vol 10(1977)4061.
2. Murawaski L., C. H. Chung & J. D. Mackenzie, *J. of Non-Cryst. Solids*, **30**, No. 2(1979)91.
3. I. G. Austin and N. F. Mott, *Adv. Phys.* Vol **18**, 17(1969)41.
4. A. Ghosh and B. K. Chaudhari, *J. of Non-Cryst. Solids* **83**(1986)151.
5. N. F. Mott, *J. of Non-Cryst. Solids* **1**(1968)1.
6. M. Sayer and A. Mansingh, *Phys. Rev. B*, **6**(1972)4629.
7. M. Sayer and A. Mansingh, J. M. Reyes & G. Rosonblatt, *J. of Appl. Phys.* **42**(1971)2857.
8. V. K. Dhawan, A. Dhawan, R. P. Tandon & J. K. Vaid, *J. of Non-Cryst. Solids* **27**(1978)308.
9. Hiroshi Hirashima, Kota Nishi & Tetsuro Yoshida, *J. of Amm. Cerm Soc.* Vol. **66**, No. 10 (1983)704.
10. Hirashi Hirashima, Daikichi Arai, Tetsuro Yoshida, *J. Amm. Ceram. Soc.* Vol. **68**, No. 9 (1985)486-489.
11. Y. Kawamoto, M. Fukuzuka, Y. Ohta & M. Imai, *Phys. & Chem. Of Glasses*, **20**, No. 3(1979)54.
12. A. Ghosh & B. K. Chaudhuri, *Indian J. Phys.* **58A**(1984)62-66.
13. G. S. Linsley, A. E. Owen & F. M. Hayatee, *J. of Non-Cryst. Solids*, **85**(1986)170.
14. Y. Dimitriev & V. Dimitriev, *Mater. Res. Bull.* **13**(1978)1071.
15. A. Mansingh, A. Dhawan, R. P. Tandon & J. K. Vaid, *J. of Non-Cryst. Solids*, **27**(1978)309.
16. H. R. Panchal and D. K. Kanchan,, *Solid State Physics (India)*, **40C**((1997)235.
17. H. Mori & H. Sakata, *J. of Mater Sci. (UK)*, **31**(1996)1621-1624.

18. H. Mori & H. Sakata, *J. of Amm. Cerm. Soc. Jpn.*, **102**(1996)562.
19. L. Murawaski, C. H. Chung & L. D. Mackenzie, *J. of Non-Cryst. Solids*, **32**(1979)208.
20. D. K. Kanchan & H. R. Panchal, *Solids Stat Physics (India)*, Vol. **41**(1998)256.
21. G. N. Greaves, *J. of Non-Cryst. Solids*, **11**(1973)427.
22. R. A. Anderson & R. K. MacCrone, *J. of Non-Cryst. Solids*, **14**(1974)112.
23. K. W. Hansen, *J. Electrochem. Soc.*, **112**(1965)1944.
24. A. W. Dozier, L. K. Wilson, E. J. Friebele, & D. L. Kinser, *J. Amm. Cerm. Soc.*, **55**(1972)373.
25. H. Hirashima & T. Yoshida,, in *Proc. 11th Int. Congress on Glass,, Prague, 1977, Vol. II*, ed. J. Gotz (North Holland, Amsterdam, 1977)p. 365.
26. T. Holstein, *Ann. Phys.* **8**(1959)325.
27. M. Sayer & A. Mansingh, *J. of Non-Cryst. Solids*, **58**(1983)91.
28. C. H. Chung, D. Lezal & J. D. Mackenzie, *J. of Mater. Sci.* **16**(1981)422.
29. B. K. Sharma, D. C. Dubey & A. Mansingh, *J. of Non-Cryst. Solids*, **65**(1984)39.
30. M. M. Ahmed & C. A. Hograth, *J. of Mater. Sci.* **18**(1983)3305.
31. C. Sanchez & J. Linage, *J. of Non-Cryst. Solids*, **65**(1984)285-300.
32. N. Suresh Rao & O. G. Palama, *Bull. Mater. Sci.* Vol. **8**, No. 3(1995)229.
33. Janakirama Rao, *J. Amm. Cerm Soc.* Vol. **48**, No. **6**(1965)311.
34. D. K. Kanchan, H. R. Panchal & A. K. Gupta, *Solid State Physics (India)*, Vol. **40c**(1997)241.
35. R. V. Anavekkr & N. Devaraj, *Phy. & Chem. Of glasses*, Vol. **32**, No.3(1991)103.

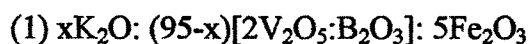
36. G. F. Lynch & M. Sayer, *J. Phys. C*, Vol. C6((1973)3661.
37. W. Chomaka, D. Samtowicz, O. Gzowski & L. Murawski, *J. of Non-Cryst. Solids*, **45**(1981)145.
38. A. K. Bandyopadhyay & J. O. Isard, *J. Phys. D, Appl. Phys.* Vol. **10**(1977)L99.
39. L. Murawski, *J. Mater.Sci.* **17**(1982)2155.
40. O. G. Palama, A. L. Shashi Mohan & A. B. Biswas, *Proc. Indian Acad. Sci. Vol. 87A*, No. 8(1978)259.
41. L. D. Bogomolova, M. P. Glassova, V. M. Kalygina, S. I. Reiman, S. N. Spasebikna & I. V. Filatova, *J. of Non-Cryst. Solids*, **85**(1986)170.
42. O. Gzowski, L. Murawski, W. Lizak, H. Binczyaka & J. Sawicki, *J. of Phys. D*, **14**(1981)L 77.
43. L. N. Kurline & Ediseeva O. N. *Keneti Katal* **14**(1973)267.
44. Burzo E. & Stanescu L., *Solid State Comm.* **20**(1976)649.

6.2 ELECTRICAL SWITCHING:

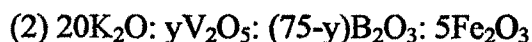
6.21 INTRODUCTION:

Transition metal oxide glasses such as $V_2O_5-P_2O_5$ ^[1-2], $K_2O-V_2O_5-BaO-ZnO$ ^[5], $V_2O_5-Fe_2O_3$ ^[4] and $V_2O_5-TeO_2$ ^[5] etc., are important due to their semiconducting nature which also show the electrical threshold as well as memory switching effects. The electrically conducting glasses are semiconducting in nature and are of technical importance in electrical and thermal switching devices. The switching is reversible and can be easily controlled in an electrical circuit. There are two types of switching; one is threshold switching and other is memory switching. Many authors have attempted upon the phenomenon of switching in past ^[6-11]. Different mechanisms have been proposed in order to explain switching process in semiconducting glasses ^[8,12-16].

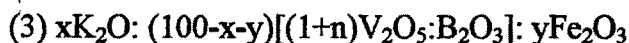
In the present study of glass system the following series has been prepared to study the switching phenomenon.



where $x=0$ to 30 in steps of 5 mole %.



where $y=40$ to 75 in steps of 5 mole %.



where $x=0$ to 20 in steps of 5 mole %.

$y=5$ to 15 mole % in steps of 2.5 mole %.

$n=1$ to 2 in step of 0.2.

For the mechanism of electrical switching, a hybrid model based on both thermal and electronic process with ambient temperature between 300-533°K has been attempted.

6.22 RESULTS AND DISCUSSION:

Typical voltage-current characteristics curves are shown in Figures 6.21, 6.22 & 6.23 for glass samples of the three series in the temperature range 300-533°K. It is observed that the samples show ohmic behaviour for low applied voltage and the current is observed to increase exponentially for intermediate voltage. When the applied voltage is further increased, a decrease in voltage drop across the sample (Figure 3.7) has been observed. This change in behaviour of the sample is termed as 'non-ohmic'. The sample has a "OFF-state" (high resistance state) at low applied voltage whereas, beyond a particular voltage, the sample has "ON-state" (low resistance state). The rapid increase in the current without significant increase in the applied voltage is considered as switching which is observed in the present glass systems. The voltage at which the non-ohmic behaviour is observed is known as "threshold voltage" represented by V_{th} or V_S ^[7,17-18]. It is observed from Figures 6.21, 6.22 & 6.23 that the voltage V_S at which the switching takes place is decreasing with the ambient temperature, which implies that the switching is a function of both voltage and temperature. Similar kind of observations were also made by Mansingh et. al.^[7] and Bansal et. al.^[19]. It can be seen from the Table 6.21 for $V_2O_5 = 63.66$ mole %, that the switching voltage V_S changes from 25 volt to 14 volt when temperature changes from 378-423°K. A Similar behaviour of decrease in switching voltage with ambient temperature has been observed in other glass samples of the two series. Hence, if the voltage at switching follows the following exponential law given by

$$V_S = V_o \exp(-\beta/kT) \quad (6.21)$$

The plots between $\ln V_S$ and $10^3/T$ should show a linear decrease of $\ln V_S$ with the rise of a temperature, which is the case in present system [Figure 6.24 (a), (b) & (c)]. Thus, it may be possible to observe switching by two means; one by adjusting the applied voltage and other by controlling the ambient

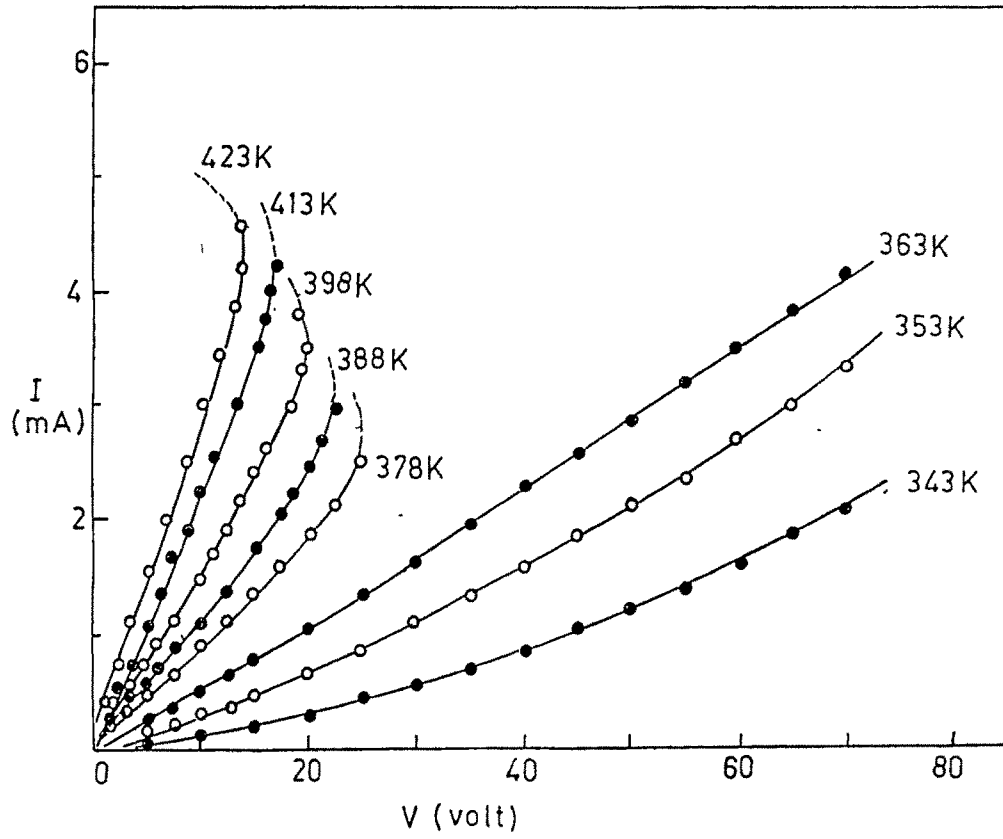


Figure 6.21 (a) : I-V characteristics for $V_2O_5 = 63.33$ mole % in series 1.

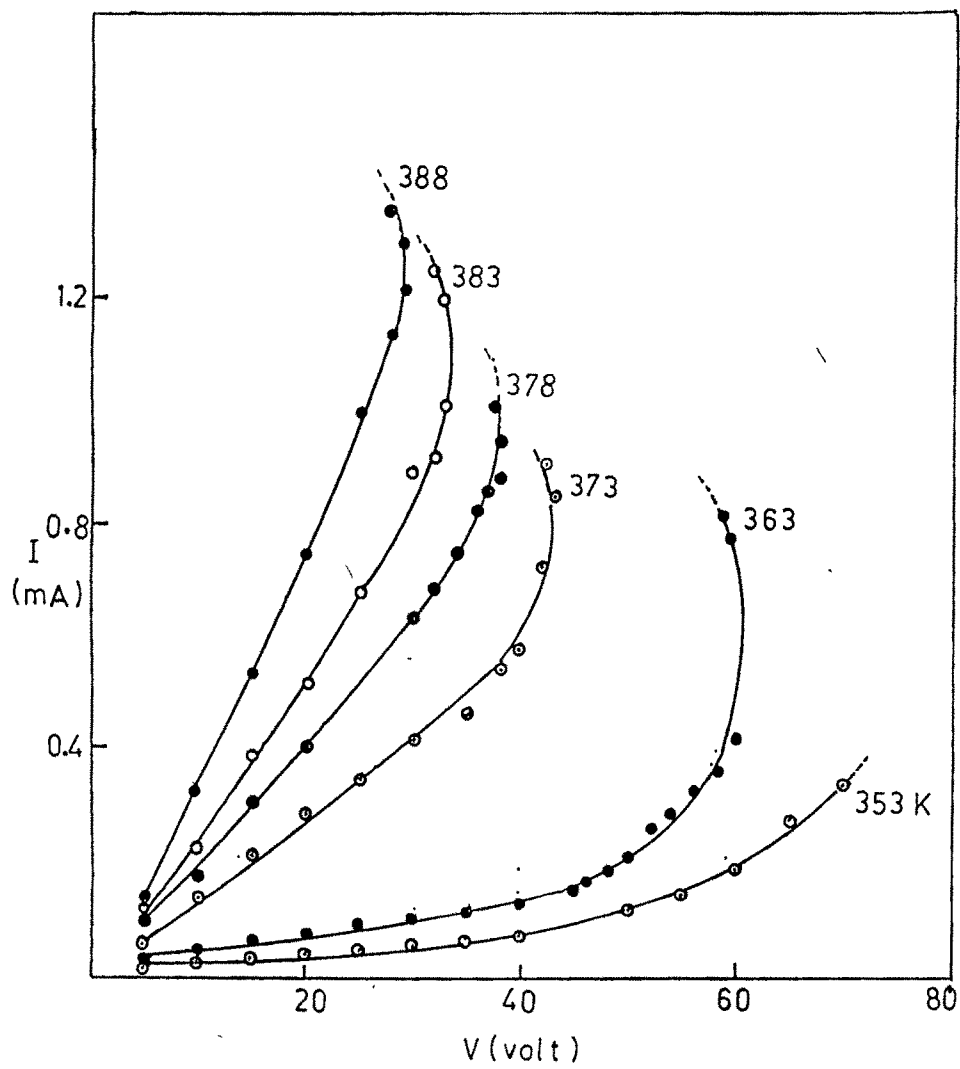


Figure 6.21 (b) : I-V characteristics for $V_2O_5 = 60$ mole % in series 1.

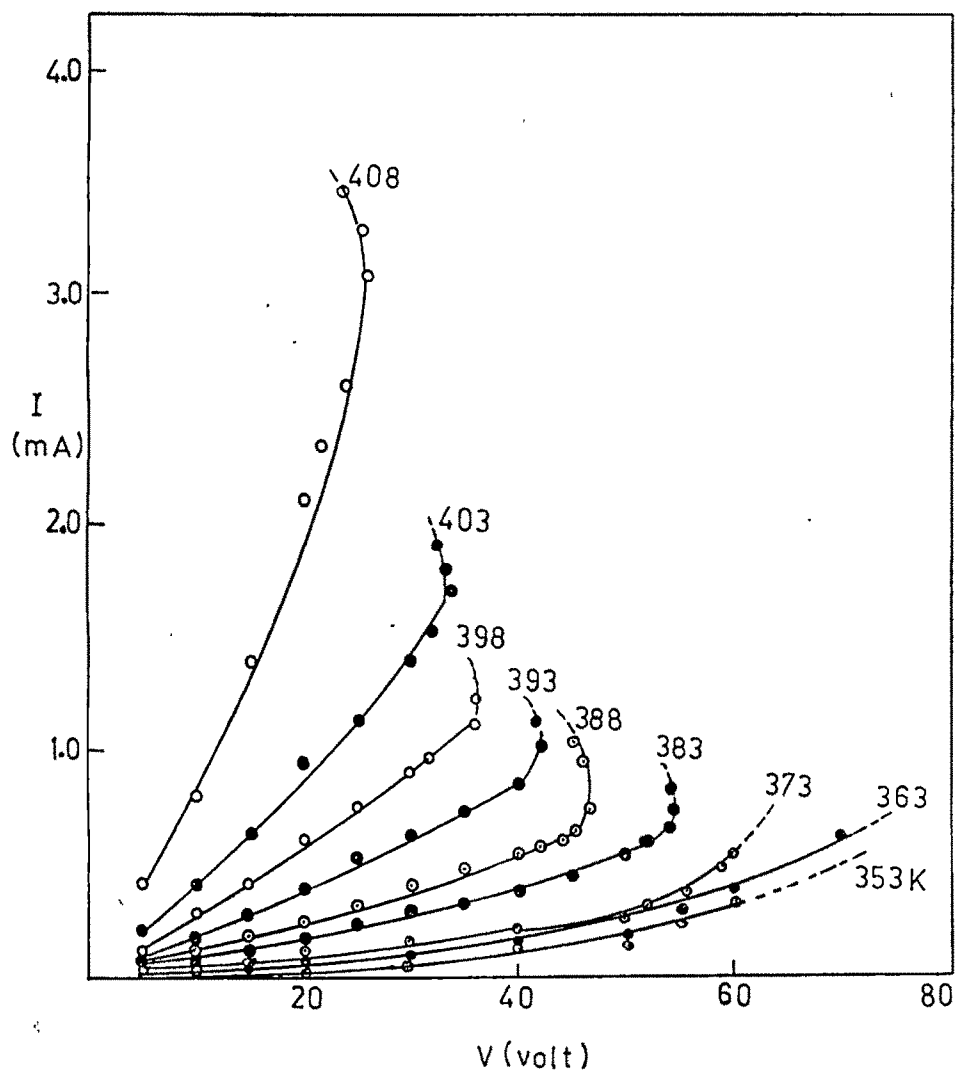


Figure 6.21 (c) : I-V characteristics for $V_2O_5 = 56.67$ mole % in series 1.

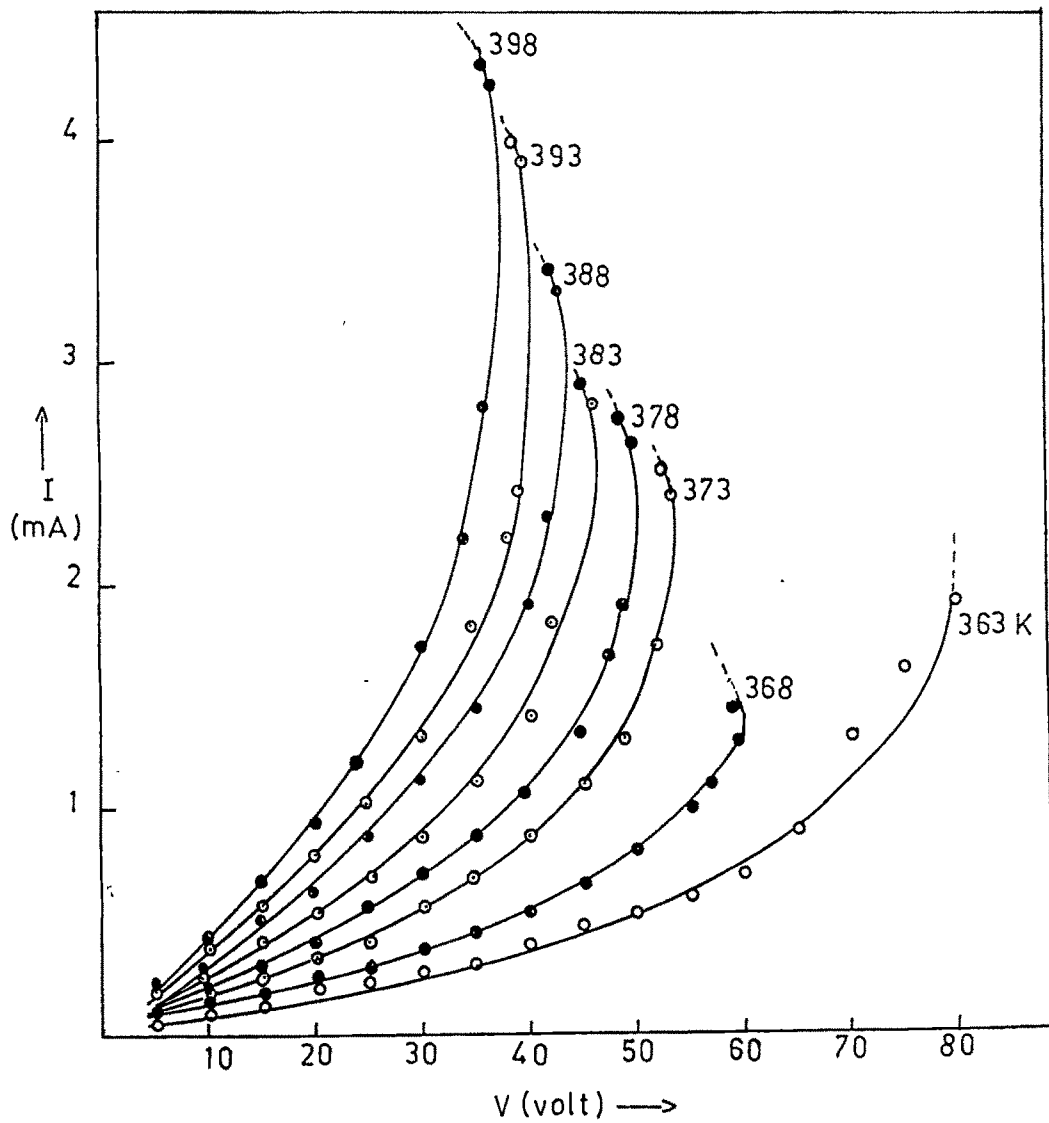


Figure 6.22 (a) : I-V characteristics for $V_2O_5 = 75$ mole % in series 2.

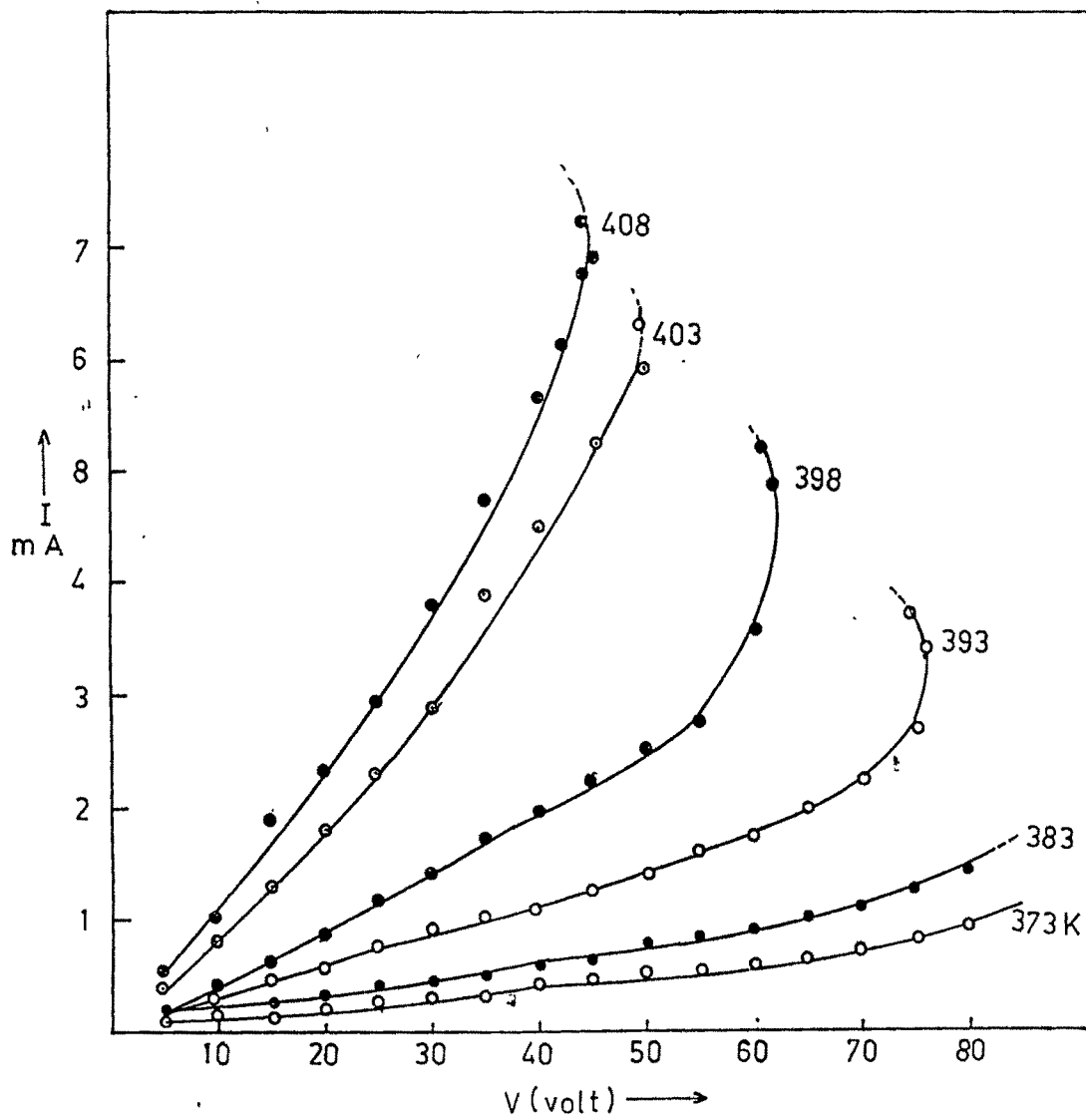


Figure 6.22 (b) : I-V characteristics for $V_2O_5 = 70$ mole % in series 2.

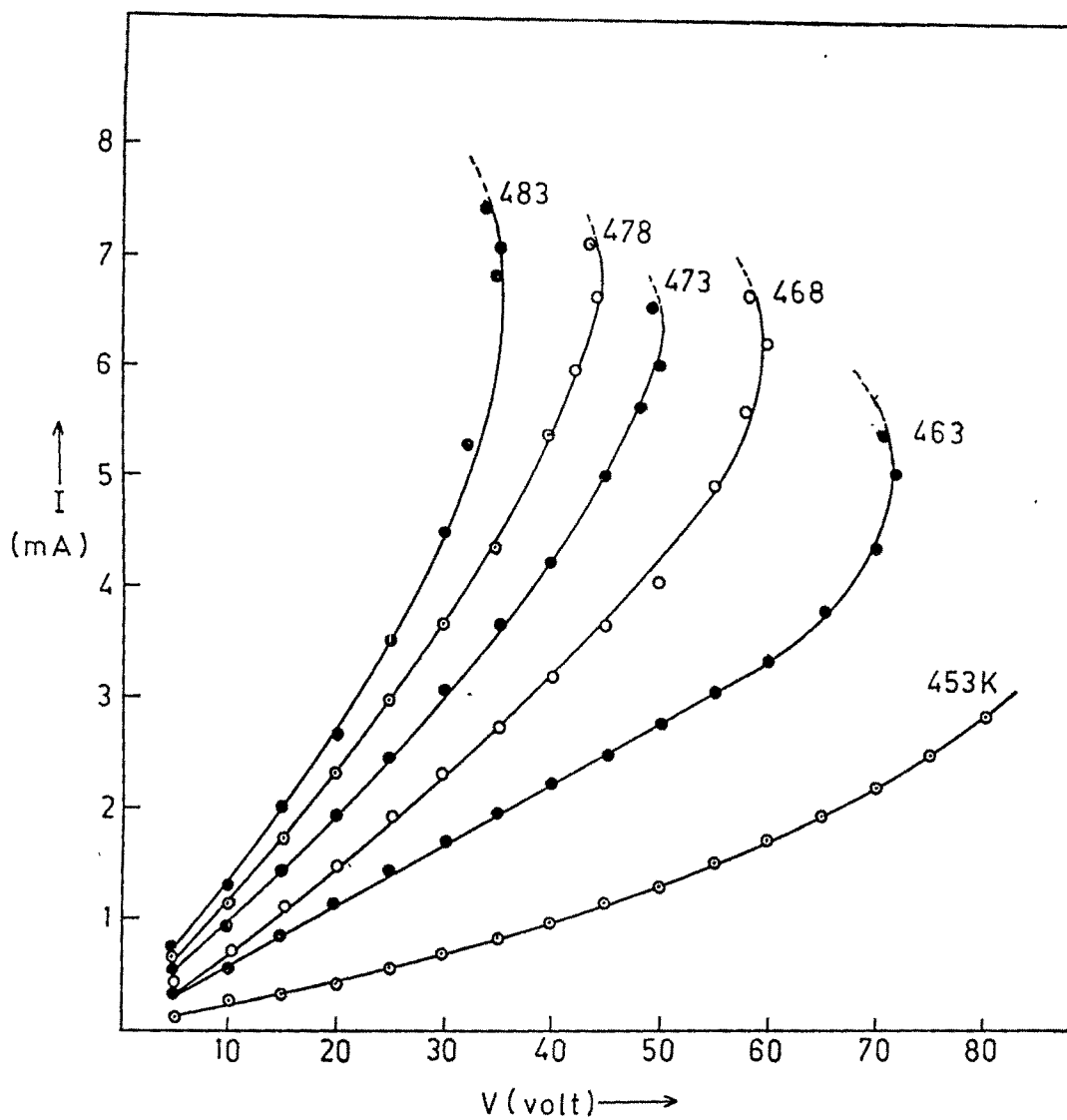


Figure 6.22 (c) : I-V characteristics for $V_2O_5 = 50$ mole % in series 2.

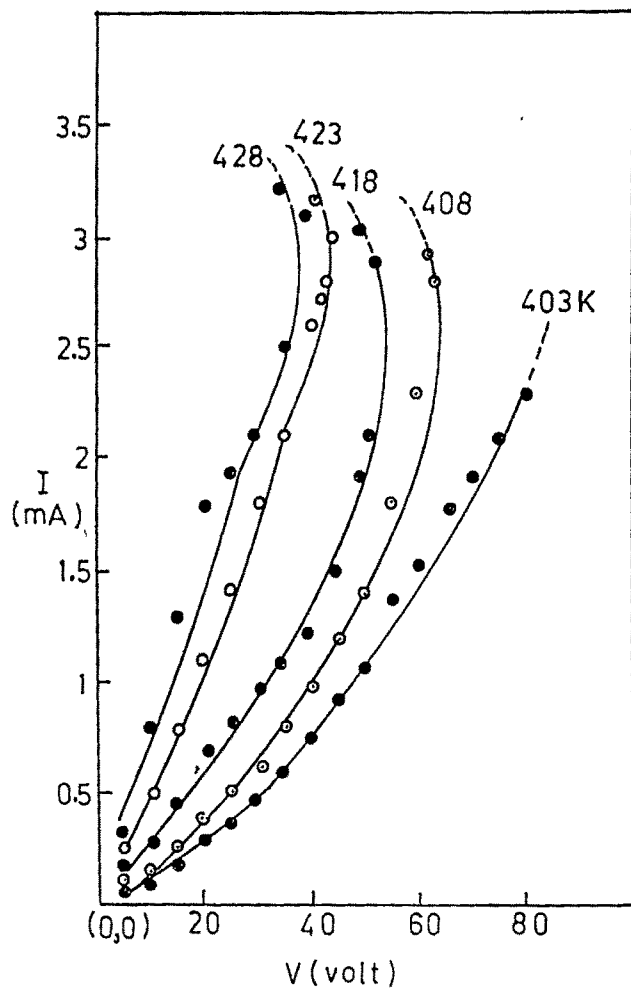


Figure 6.23 (a): I-V characteristics for $V_2O_5 = 49.23$ mole % in series 3.

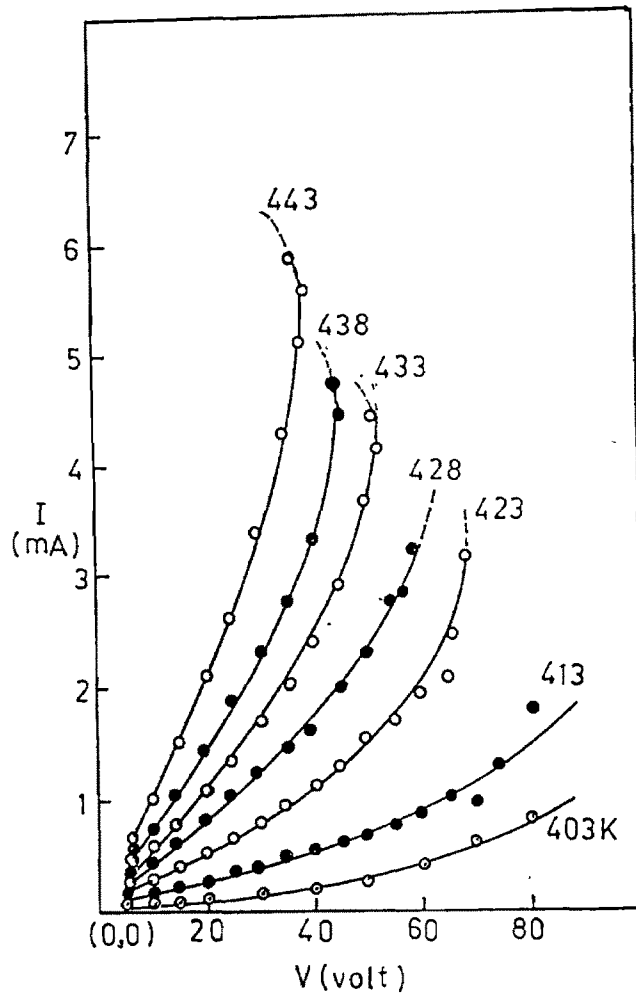


Figure 6.23 (b): I-V characteristics for $V_2O_5 = 46.67$ mole % in series 3.

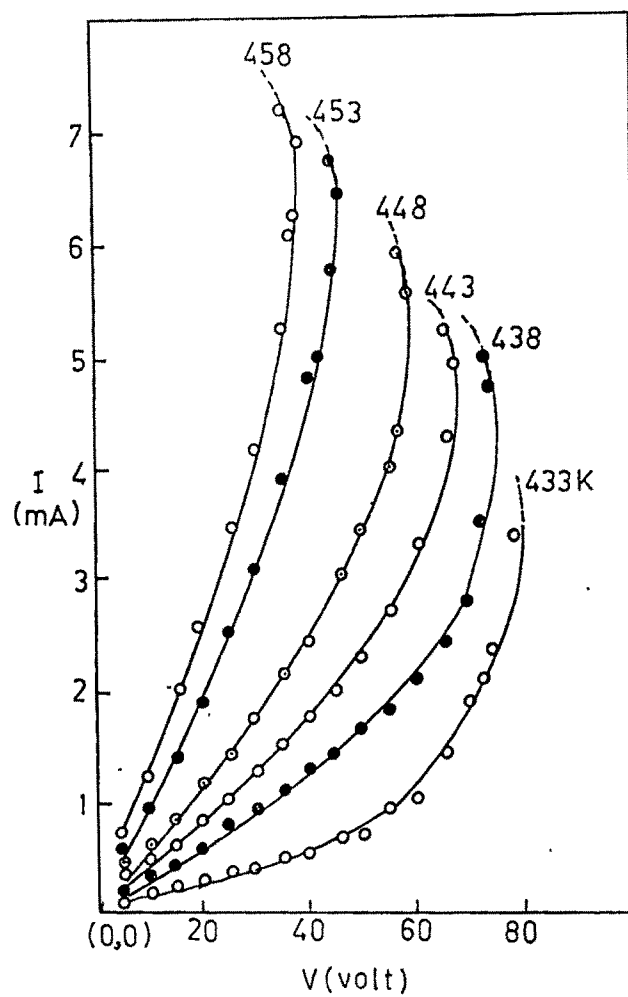


Figure 6.23 (c): I-V characteristics for $V_2O_5 = 43.33$ mole % in series 3.

Table : 6.21 : Switching Data for $xK_2O : (95-x)[2V_2O_5 : B_2O_3] : 5 Fe_2O_3$

V_2O_5 %	T (°K)	Vs (Volt)	Rs KΩ	T _D (°K)	Ts (°K)	Power (Watt)	Current I _S (mA)	Radiation loss (f)
63.33	378.0	25	10.2	514.5	469.7	0.061	2.45	4.97×10^{10}
	388.0	23	7.96	528.8	510.5	0.066	2.89	5.55×10^{10}
	398.0	20	5.6	550.3	527.9	0.071	3.56	6.66×10^{10}
	413.0	17	4.0	572.1	543.5	0.072	4.2	7.80×10^{10}
	423.0	14	3.1	591.9	555.5	0.064	4.56	9.08×10^{10}
60	363.0	60	140.2	365.7	376.2	0.026	0.43	5.24×10^8
	373.0	43	50.2	397.0	397.4	0.035	0.86	5.49×10^8
	378.0	38	39.6	405.1	392.6	0.036	0.96	6.49×10^8
	383.0	33	30.6	414.4	399.1	0.036	1.08	7.91×10^8
	388.0	29	23.8	423.4	401.1	0.037	1.22	9.48×10^8
56.67	383.0	54	82.4	403.2	396.5	0.035	0.66	4.91×10^9
	388.0	47	61.8	413.0	401.3	0.036	0.76	6.43×10^9
	393.0	42	38.9	429.9	406.0	0.045	1.08	1.08×10^{10}
	398.0	36	31.3	438.3	403.5	0.041	1.15	1.18×10^{10}
	403.0	34	19.7	457.5	408.8	0.059	1.73	1.74×10^{10}
408.0	26	8.4	497.2	434.9	0.081	3.1	3.20×10^{10}	

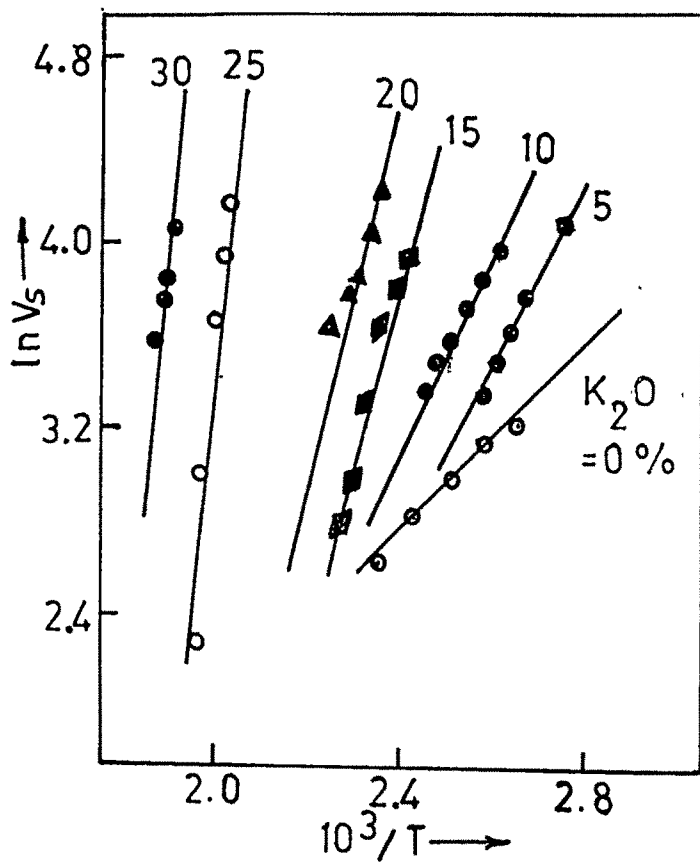


Figure 6.24 (a) : Plot of $\ln V_s$ versus $10^3/T$ for series 1.

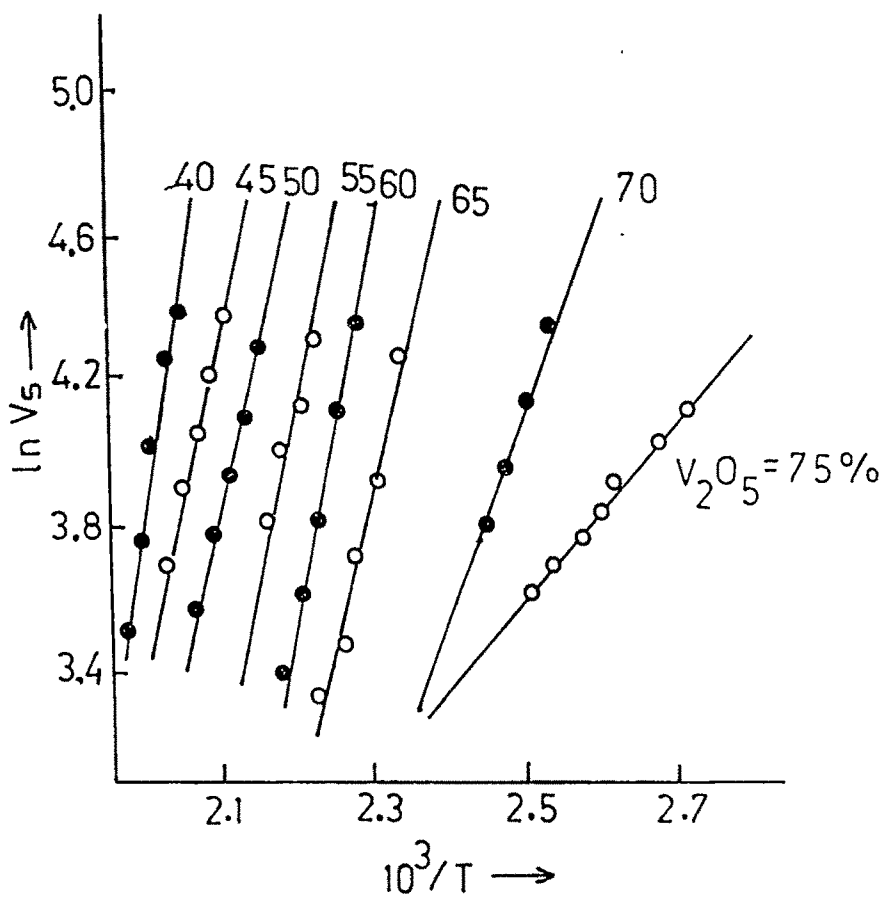


Figure 6.24 (b) : Plot of $\ln V_s$ versus $10^3/T$ for series 2.

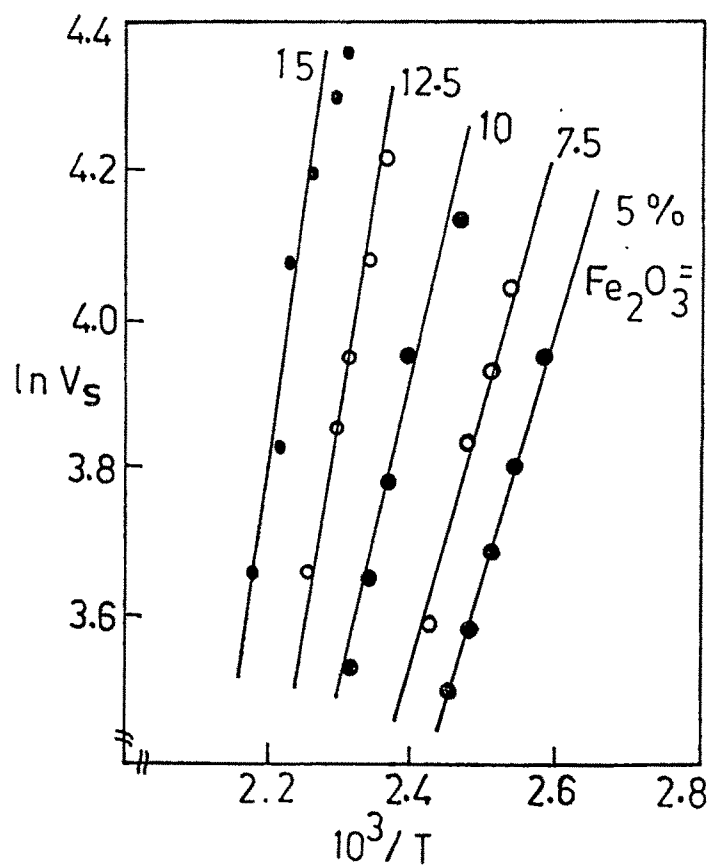


Figure 6.24 (c) : Plot of $\ln V_s$ versus $10^3/T$ for series 3.

temperature of the sample. It can be seen from the above Figures and Tables that before the switching takes place in the sample, the ambient temperature and the switching temperatures of the samples are equal. At the time of switching, the sample temperature for the same glass sample (for $V_2O_5=63.33$ mole % in series 1) increases from 378 °K to 469 °K. Also, the resistance of the glass sample, before switching, remains constant and decreases at the time of switching. The dependence of the resistance of the glass sample on the ambient temperature was also discussed by various authors^[20-21]. The resistance of the sample for $V_2O_5= 63.33$ mole % in series-1 at 378 °K is 10.2 k Ω , which decreases to 3.1 k Ω at the switching temperature. Similarly for $V_2O_5 =70$ mole % in series 2 (Table 6.22), the resistance of the sample at 393 °K is 21.8 k Ω , which decreases to 6.5 k Ω at 408 °K and for $V_2O_5 = 46.67$ mole % in series 3 (Table 6.23), the resistance of the glass sample decreases from 21.5 k Ω to 6.9 k Ω with the change of temperature from 423 °K to 443 °K. Obviously, the resistance of the glass sample at switching (R_s) also follows the exponential law given by;

$$R_s = R_o \exp(W/kT) \quad (6.22)$$

The resistance at switching of the glass sample decreases exponentially with increase of the ambient temperature. It is observed that the ratio of the 'OFF-state' (before switching) to 'ON-state' (at switching) static resistance decreases with increasing the ambient temperature. At higher ambient temperature, the switching current is also observed to be high, which requires a more electrical "power input" which inturn decreases the resistance of the glass sample at switching^[19].

The temperature at which the switching is observed for all glass samples is calculated by using the following relation by knowing the values of k, W, R and R_s at a given ambient temperature.

$$\frac{1}{T_s} = \frac{1}{T} - \frac{k}{W} \ln\left(\frac{R}{R_s}\right) \quad (6.23)$$

Table : 6.22 : Switching Data for 20K₂O: yV₂O₅: (75-y)B₂O₃ : 5 Fe₂O₃

V ₂ O ₅ %	T(°K)	V _s Volt	R _s KΩ	T _D (°K)	T _S (°K)	Power (Watt)	Current I _S (mA)	Radiation loss (f)
75	368.0	61	29.1	382.9	392.1	0.128	2.1	3.17 x 10 ⁹
	373.0	53	21.6	393.5	400.8	0.130	2.45	3.44 x 10 ⁹
	378.0	50	18.8	393.5	405.7	0.133	2.66	3.55 x 10 ⁹
	383.0	46	16.4	399.2	409.7	0.129	2.8	3.88 x 10 ⁹
	388.0	43	12.8	405.5	416.8	0.144	3.35	4.38 x 10 ⁹
	393.0	40	10.1	410.7	425.2	0.158	3.95	4.58 x 10 ⁹
	398.0	37	8.7	416.7	429.9	0.158	4.26	5.05 x 10 ⁹
70	393.0	76	21.8	434.3	386.4	0.264	3.48	1.17 x 10 ¹⁰
	398.0	62	12.5	439.9	403.0	0.307	4.95	1.24 x 10 ¹⁰
	403.0	52	9.6	448.5	409.4	0.283	5.44	1.40 x 10 ¹⁰
	408.0	45	6.5	451.1	425.3	0.314	6.98	1.37 x 10 ¹⁰
50	463.0	72	14.4	540.7	463.0	0.361	5.01	3.95 x 10 ¹⁰
	468.0	60	9.7	545.5	479.0	0.371	6.19	4.06 x 10 ¹⁰
	473.0	51	8.0	557.7	481.7	0.324	6.35	4.67 x 10 ¹⁰
	478.0	44	6.7	565.8	487.6	0.290	6.58	5.02 x 10 ¹⁰
	483.0	35	4.9	578.8	498.9	0.247	7.05	5.32 x 10 ¹⁰

Table : 6.23 : Switching Data for $xK_2O:(100-x-y)[(1+n)V_2O_5: B_2O_3]:yFe_2O_3$.

V_2O_5 %	T(°K)	V _s Volt	R _s KΩ	T _D (°K)	T _S (°K)	Power (Watt)	Current I _s (mA)	Radiation loss (f)
49.23	418.0	52	17.9	467.1	420.5	0.150	2.9	1.71×10^{10}
	4230	44	14.7	476.8	424.5	0.132	3	1.97×10^{10}
	428.0	39	12.6	481.8	430.9	0.121	3.1	2.03×10^{10}
	433.0	34	8.7	487.2	440.1	0.133	3.9	2.12×10^{10}
	438.0	30	6.7	489.8	453.3	0.135	4.5	2.07×10^{10}
46.6	423.0	68	21.5	441.9	478.9	0.215	3.20	2.06×10^{10}
	433.0	52	12.5	458.9	501.5	0.216	4.16	2.81×10^{10}
	438.0	47	9.1	453.7	515.5	0.244	5.19	3.91×10^{10}
	443.0	39	6.9	458.3	528.9	0.221	5.66	3.98×10^{10}
43.33	433.0	78	23.9	448.0	526.8	0.261	3.35	4.19×10^{10}
	438.0	74	15.7	463.9	545.9	0.348	4.7	5.21×10^{10}
	443.0	67	13.7	464.0	553.3	0.329	4.9	5.52×10^{10}
	448.0	59	10.5	471.0	567.2	0.330	5.6	6.32×10^{10}
	453.0	46	7.1	469.1	589.5	0.298	6.46	7.86×10^{10}
	458.0	39	5.7	473.5	603.3	0.268	6.88	8.85×10^{10}

Where R_s is the resistance of the sample at switching and R is the resistance at T for low applied field. The switching temperature was measured by using Cr-Al thermocouple in contact with the glass sample (Figure 3.7).

It is clear from the observations given in Tables 6.21, 6.22 and 6.23, the switching temperature, T_s , increases with increase of the ambient temperature. Following may be the reason for dependence of V_s and T_s on temperature and composition as well.

(i) To observe the switching at any desired ambient temperature, sufficient power is to be given so as to raise the sample temperature from T to T_s and T_s is expected to increase with ambient temperature due to sufficient Joule's heating. For $V_2O_5 = 63.33$ mole %, in series-1, the switching is observed at 25 volt at 378 °K and required input power is 0.061 watt. If the temperature is raised to 413 °K, the electrical input power increases to 0.072 watt.

(ii) With the increase of glass modifier K_2O in glasses of series 1, the V-V spacing is expected to increase, which decreases the conductivity of the glass samples^[22-23]. For the glasses in series 2, keeping modifier K_2O constant, the V-V spacing decreases because the glass former ratio V_2O_5/B_2O_3 increases and an increase in conductivity is expected. In case of third series, both the amount of K_2O and Fe_2O_3 are varied, which further increase the spacing between vanadium ions in the structure and give rise to the same decrease in the conductivity^[22,24-25]. Thus, a decrease in conductivity (or increase of the resistivity) requires more electrical power input; which raises the sample temperature from T to T_s , which also decreases the switching voltage, V_s , and increases the switching current. Figures 6.25 (a), (b) & (c) show the change in the switching temperature, T_s , with composition. Mansingh et. al.^[12] discussed that the switching voltage, V_s , and the switching current are also composition dependent. It can be seen that the switching voltage decreases and switching current increases with increasing the V_2O_5 amount in the glass samples. For glass series-1 (Table-6.21), at a given temperature 388K, the switching voltage

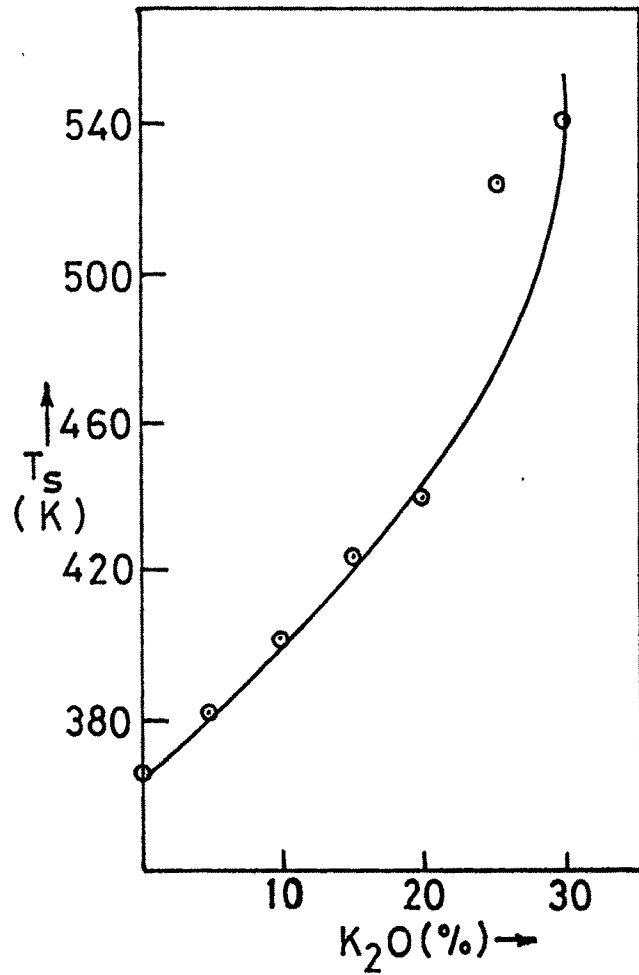


Figure 6.25 (a) : Plot of T_s versus K_2O mole % for series 1.

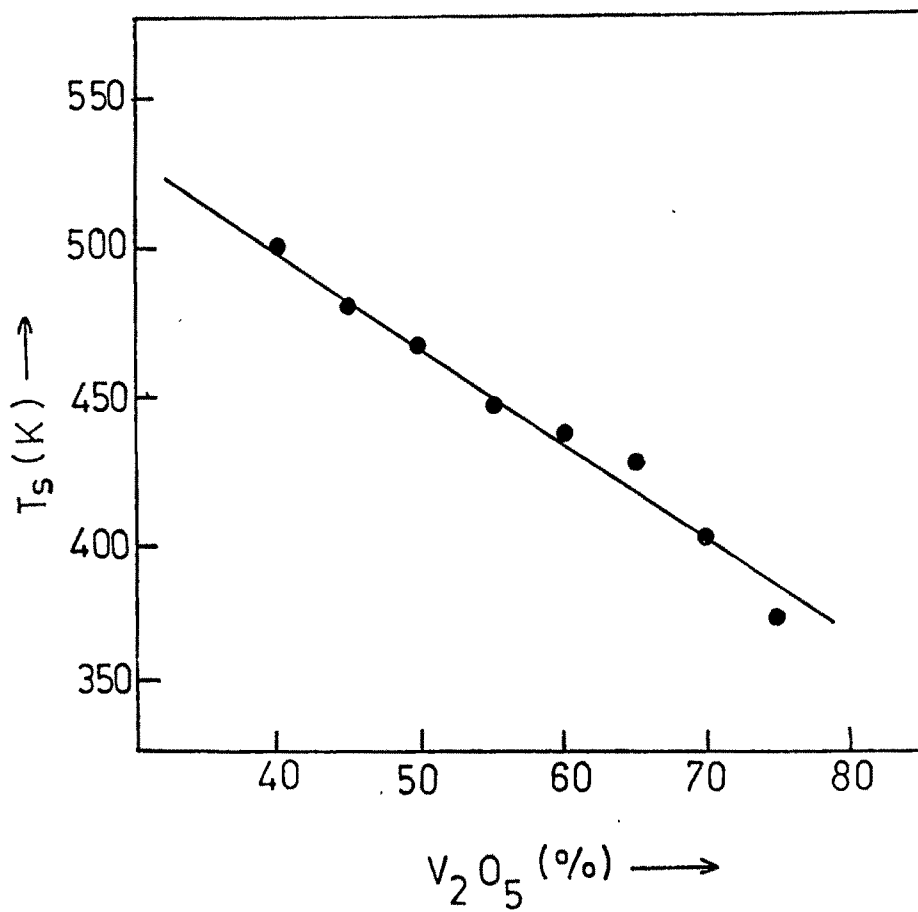


Figure 6.25 (b) : Plot of T_s versus Fe_2O_3 mole % for series 2.

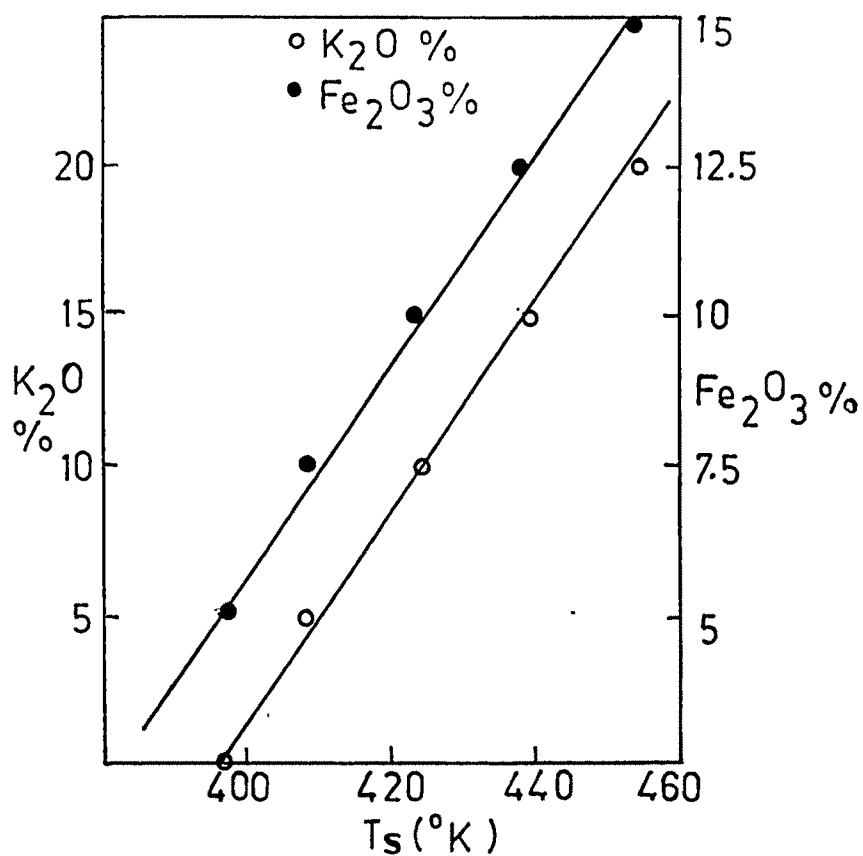


Figure 6.25 (c) : Plot of $\ln T_g$ versus Fe₂O₃ mole % for series 3.

decreases from 47 to 23 volt with increasing V_2O_5 amount from 56.67 to 63.33 mole %. In the other words, by increasing the V_2O_5 in the glass sample, switching can be achieved at the same ambient temperature at lower applied voltage. It can be seen from the Tables 6.21 to 6.23 that by changing the glass composition, the temperature of the sample at switching increases with increasing T. It is also observed that the sample temperature, (T_D), becomes greater than the ambient temperature as the current increases in the sample near the switching process because of the flow of higher current. If there is a difference in the temperature of the sample and environment (ambient), in thermal equilibrium, following Stefan-Boltzmann law, the radiation from the sample may take place and the radiation loss may be given by;

$$T_D^4 - T^4 = f \quad (6.24)$$

where f is a measure of radiation loss from the sample and is expected to be a function of electrical input power $P = I \cdot V$. It is clear from Tables that the radiation loss from the glass samples increases with increasing the ambient temperature. Thermal model suggested by B. Fisher^[21] and Yu R. J.^[26] assumes that at switching the temperature of the entire sample reaches to the glass transition temperature T_g . In the present study of I-V characteristics, the current was very high at switching and some of the samples peel off in few of the observations. This may be due to the increase of the sample temperature beyond the glass transition temperature and the sample is destroyed. These radiation losses are supposed to increase with the increase of ambient temperature because higher is the ambient temperature higher is the difference between the temperature of the sample near switching and ambient. To compensate these radiation losses, more electrical power is needed to maintain that difference of temperature.

Treating the radiation loss f as a power series in P, the equation can be expressed as;

$$f = \alpha_0 + \alpha_1 P + \alpha_2 P^2 + \dots + \alpha_N P^N \quad (6.25)$$

If the "power-input" equals to zero, it is expected that $T_D=T$ and the constant α_0 is expected to be zero. Solving Equation 6.22 and 6.25 we can write

$$f = \left[\frac{W}{k \ln \left(\frac{R}{R_s} \right)} \right]^4 - T^4 \quad (6.26)$$

The radiation loss from the sample is calculated from the experimental values of W , R and R_0 for a given temperature T . As the values of input power P are known, f can be calculated from Equation 6.25 provided the coefficient $\alpha_1, \alpha_2, \alpha_3, \dots, \alpha_N$ are also known. The values of the coefficients $\alpha_1, \alpha_2, \alpha_3, \dots, \alpha_N$ are calculated by using the method of sum of deviations of f values to give a minimum value of

$$\sum_{\text{all data points}} \left| f_{\text{Equation 6.25}} - f_{\text{Equation 6.26}} \right| = \text{Minimum}$$

The values of $\alpha_1, \alpha_2, \alpha_3, \dots, \alpha_N$ were worked out by computer fitting the above polynomials. After knowing the coefficients $\alpha_1, \alpha_2, \alpha_3, \dots, \alpha_N$, the voltage across the sample (theoretically) can be computed for any current I by the following equation.

$$V_{\text{cal}} = IR_0 \exp \left[\frac{W}{k(T^4 + \alpha_1 P + \alpha_2 P^2 + \dots)^{1/4}} \right] \quad (6.27)$$

The calculated values of the coefficient of voltage V_{cal} are found to be in good agreement with experimental values which proves the present model for thermal switching envisaged for the present glass system.

Hence, from the present study, the following observations have been made.

- (i) The switching voltage, V_s , and switching temperature, T_s , has been found composition dependent.

- (ii) The resistance of the sample at a given ambient temperature remains constant (OFF-state) and found to decrease at the time of switching (ON-state), which is also temperature dependent.
- (iii) For sufficient Joule's heating more electrical power is required, which increases the switching temperature and decreases the switching voltage. Also, the radiation loss from the sample is expected to increase with increasing the ambient temperature.
- (iv) The above thermal model for thermal switching has been attributed due to Joule's heating fits well for the present glass system.
- (v) The present devices can be used as a voltage as well as thermal switches.

REFERENCES:

1. M. Sayer and A. Mansingh, Phys. Rev. B, **6**(1972)4629.
2. M. Sayer and A. Mansingh, J. M. Reyes & G. Rosonblatt, J. of Appl. Phys. **42**(1971)2857.
3. Y. Kawamoto, M. Fukuzuka, Y. Ohta & M. Imai, Phys. & Chem. Of Glasses, **20**, No. 3(1979)54.
4. R. V. Anavekkr & N. Devaraj, Phy. & Chem. Of glasses, Vol. **32**, No.3(1991)103.
5. R. A. Anderson & R. K. MacCrone, J. of Non-Cryst. Solids, **14**(1974)112.
6. C. F. Darke, L. F. Scanlan and A. Engel., Phys. Stat. Solidi, **32**(1969)193.
7. A. Mansingh and R. Singh, J. Phys. C., **13**(1980)5725.
8. A. Mansingh, R. Singh & S. B. Krupanidhi, Solid. Stat. Electron, **23**(1980) 649.
9. H. J. Stocker, C. A. Barlow, Jr. D. F. Weirauch, J. Non. Cryst. Solids **4**(1970)523.
10. S. R. Ovshinsky, Phys. Rev. Lett. (USA), Vol. **21**, No.24(1968)1632.
11. A. Mansingh, J. K. Vaid & R. P. Tandon, Phys. Stat. Solid. (a) **38**(1976) K1.
12. A. Mansingh and V. K. Dhavan, Phil. Mag. B. **47**(2)(1983)121-138.
13. B. W. Flynn & A. E. Owen, J. De Phys. C**4**(1981)1005.
14. N. F. Mott, Contemp Phys. **10**(1969)125.
15. N. F. Mott, Phil Mag. **24**(1971)911.
16. W. Van Roosbroeck, J. of Non-Cryst. Solids, **12**(1973)232.
17. A. A. Hosseini & C. A. Hogarth, J. Mater. Sci. **20**(1985)261-268.
18. S. R. Jones, M. J. Thompson, J. Allison & R. F. Ormendroy, J. Non-Cryst. Solids, **28**(1978)1-21.
19. T. K. Bansal, S. Bansal & R. G. Mendiratta, J. of Non-Cryst. Solids., **99**(1983)168.

20. J. K. Higgins, B. K. Temple & J. E. Lewis, *J. Non. Cryst. Solids*, **23**(1977)187.
21. B. Fisher, *J. Phys. C., Solid State Phys.* **8**(1975)2072.
22. H. R. Panchal, D. K. Kanchan & D. R. S. Somayajulu, *J. Mater. Sci. Forum* (UK), Vol. **223-224**(1996)301.
23. C. Sanchez & J. Linage, *J. of Non-Cryst. Solids.*, **65**(1984)285-300.
24. I. G. Austin & N. F. Mott, *Adv. Phys.* **18**(1969)41.
25. H. R. Panchal & D. K. Kanchan, *Solid State. Physics(India)*, **39C**(1996)218.
26. R. J. Yu & P. D. Fisher, *Appl. Phys. Lett.*, **19**(1971)158.

6.3 THERMOELECTRIC STUDIES:

Most of the glasses containing transition metal ions are semiconductors and it is well established that conduction in these glasses is due to the transfer of electrons from a lower valence state to a higher valence state^[1-2]. Thermal power data for vanadium and some compositions of tungsten phosphate glasses have been reported^[2-4]. thermoelectric power measurement on $\text{WO}_3\text{-P}_2\text{O}_5$, $\text{V}_2\text{O}_5\text{-P}_2\text{O}_5$, $\text{MoO}_3\text{-P}_2\text{O}_5$ ^[5], $\text{V}_2\text{O}_5\text{-Sb}_2\text{O}_3\text{-TeO}_2$ and $\text{V}_2\text{O}_5\text{-Bi}_2\text{O}_3\text{-TeO}_2$ ^[6], $\text{V}_2\text{O}_5\text{-BaO-K}_2\text{O-ZnO}$ ^[7] and $\text{K}_2\text{O-V}_2\text{O}_5\text{-B}_2\text{O}_3\text{-Fe}_2\text{O}_3$ ^[8] were carried out in the past. The thermoelectric power measurements were carried out for the glass samples of the series 1,2 and 3 in the temperature range 300 °K to 425 °K. Figures 6.31 (a), (b) & (c) show the relation between thermoelectric power, Q , and the temperature, T , from 300 °K to 425 °K for all the glasses for first, second and third series respectively. It can be seen that thermoelectric power, Q , is independent of temperature for a given glass composition. A similar behaviour is observed for $\text{V}_2\text{O}_5\text{-Sb}_2\text{O}_3\text{-TeO}_2$ and $\text{V}_2\text{O}_5\text{-Bi}_2\text{O}_3\text{-TeO}_2$ ^[6] glass systems. However, the negative sign appeared in thermoelectric power, Q , for all glass samples which indicates that these glasses have n-type semiconducting nature^[5-7]. Figures 6.32 (a), (b) & (c) represent the dependence of thermoelectric power, Q , on the composition. It is observed from these figures that thermoelectric power increases with increase of K_2O and Fe_2O_3 concentration in series 1 and 3 respectively, whereas the value of Q decreases with the increase of concentration of the V_2O_5 in glasses of series 2. The measured values of thermoelectric power, Q , in temperature range of 300 °K to 425 °K lie in the range of $-359.93 \mu\text{V}/^\circ\text{K}$ to $282 \mu\text{V}/^\circ\text{K}$, $-196.32 \mu\text{V}/^\circ\text{K}$ to $360.13 \mu\text{V}/^\circ\text{K}$ and $-333 \mu\text{V}/^\circ\text{K}$ to $-302 \mu\text{V}/^\circ\text{K}$ for first, second and third series respectively. The measured values of Q are found to be in good agreement with the earlier reported work^[5-7,9-10], for semiconducting glasses. Thermoelectric power of transition metal oxide (TMO) glasses are dependent

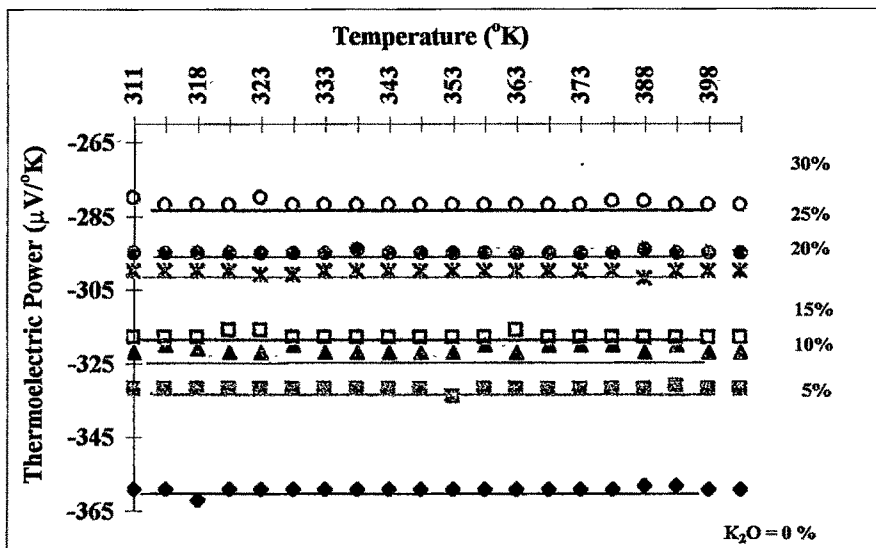


Figure 6.31 (a): Plot of Thermoelectric Power Q ($\mu\text{V}/^\circ\text{K}$) versus T ($^\circ\text{K}$) for series 1.

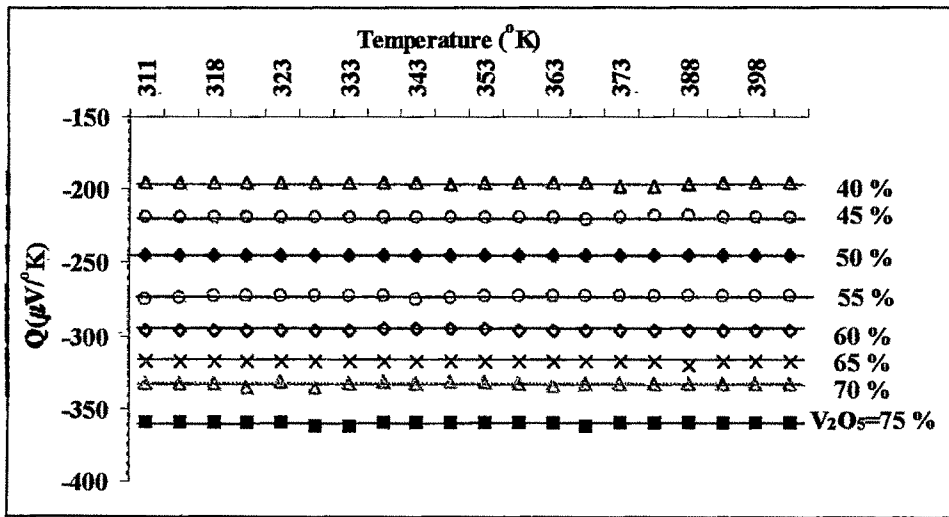


Figure 6.31 (b): Plot of Thermoelectric Power Q ($\mu\text{V}/^\circ\text{K}$) versus T ($^\circ\text{K}$) for series 2.

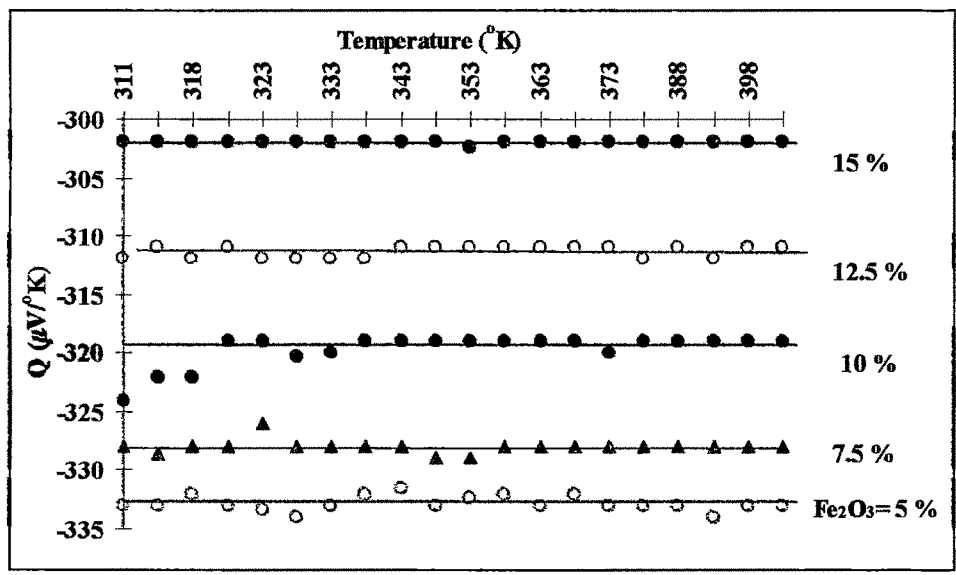


Figure 6.31 (c) : Plot of Thermoelectric Power Q ($\mu\text{V}/^\circ\text{K}$) versus T ($^\circ\text{K}$) for series 3..

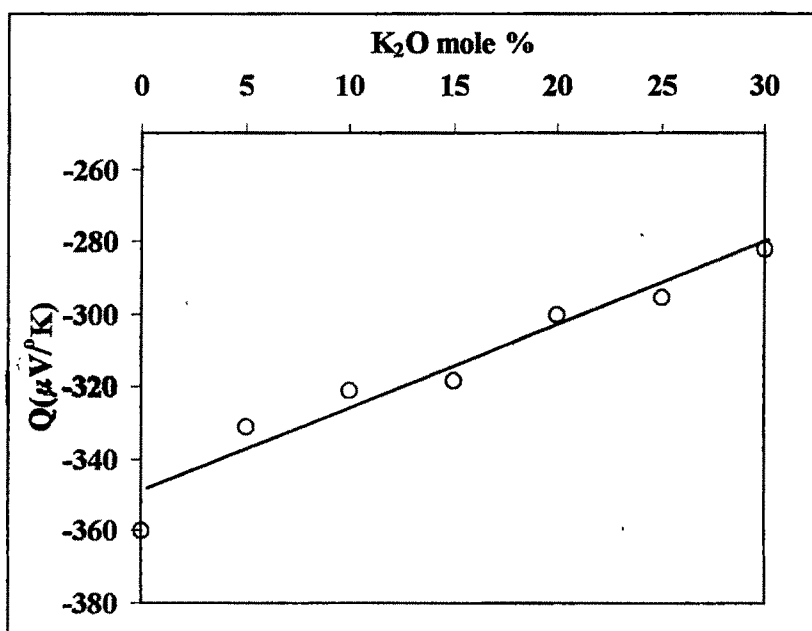


Figure 6.32 (a): Plot of $Q(\mu V/K)$ versus K_2O mole %.

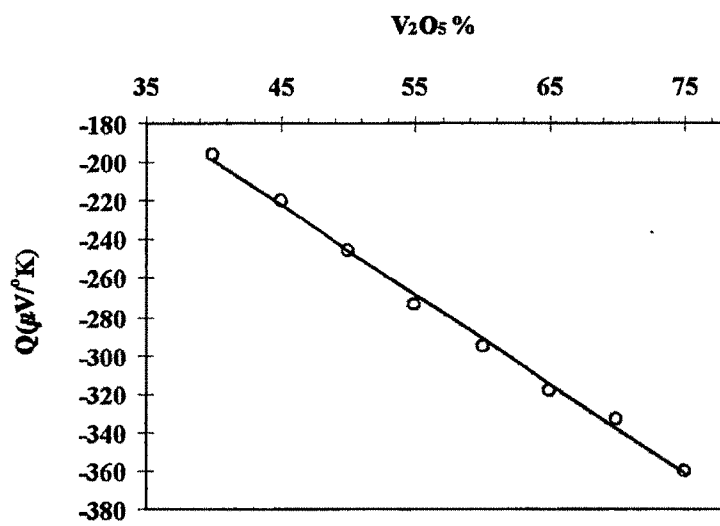


Figure 6.32 (b) : Plot of $Q(\mu\text{V}/\text{K})$ versus V_2O_5 mole %.

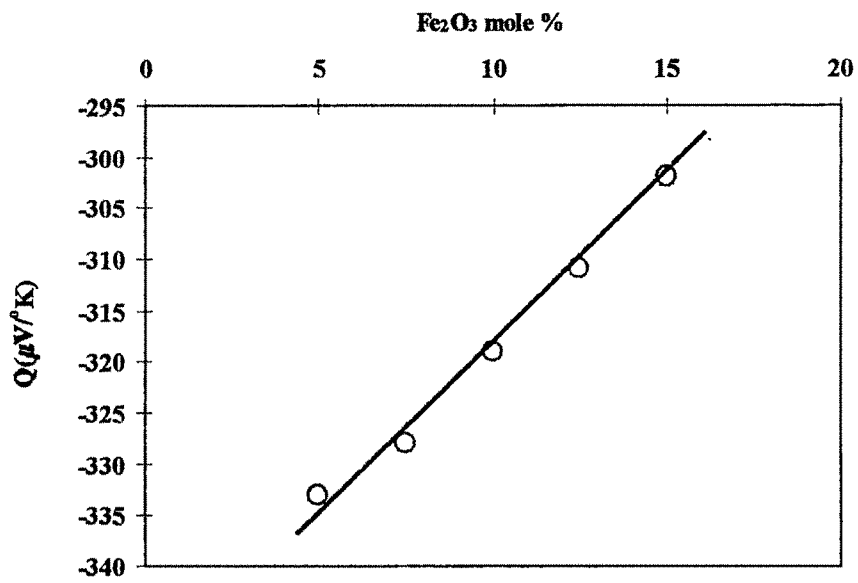


Figure 6.32 (c) : Plot of $Q(\mu\text{V}/\text{K})$ versus Fe_2O_3 mole %.

on the ratio of concentration of reduced transition metal ions to total transition metal ions, C_V , i.e., V^{+4}/V_{total} . The thermoelectric power of the semiconducting glass system has been calculated by using Heikes and Ure formula ^[11-12].

$$Q = \left(\frac{k}{e} \right) \left[\ln \frac{C_V}{1 - C_V} + \alpha' \right] \quad (6.31)$$

In Heikes formula C_V is the ratio of low valence state V^{+4} to V_{total} , α' is the constant of proportionality between heat of transfer and the kinetic energy of electrons. It has been suggested by Appel J.^[13] and Austin I. G. And Mott^[14] that for $\alpha' \gg 2$ is applicable for large polarons. For narrow band semiconductors with small polaron formation, the polaron band width (J_p) is very much smaller than kT ^[2,14]. Due to localization of electrons and their low mobility, the heat of transfer should be small compared to kT and constant α' should be much smaller than one.

In case of band polarons, a value of zero for α' has been suggested by Appel J.^[13], Sewell G. L.^[15] and Klinger M. I.^[16] and indicating that the thermal power should depend only on C_V and should be independent of the temperature. If C_V is independent of temperature as in transition metal oxide glasses^[17] then Q is expected to be independent in the present glass system. Hence, Figures 6.31 (a), (b) and (c) suggest that Q is independent of temperature hence C_V is also independent of temperature.

However, Austin and Mott^[14] have suggested that the α' term can be zero only if disorder energy in the system is zero. If there is a disorder energy between the occupied and unoccupied sites, then the α' term should be finite not zero. The measured values of thermal power Q , and calculated values of α' for different glasses of all the three series are reported in Table 6.31. The ratio c of reduced valency state to the total number of transition metal ions, disorder energy, W_D , activation energy, W , are also reported in the Table 6.31.

As it can be seen from Heikes formula (Equation 6.31) that the slope of line between Q and $\ln(C_V/1-C_V)$ is equal to $k/e = -86.18 \mu V/^\circ K$ and the value of

Table 6.31 : Data of Thermoelectric power measurement for series 1,2 & 3.

	Mole %	W (eV)	W _H (eV)	W _B (eV)	Q _{expt} μV/K	Q _{cal} μV/K	V ⁴ x 10 ²⁰	V ⁵ x 10 ²⁰	V ⁴ /V _{total}	α'	θ	lnV ⁵ /V ⁴
Series 1	K ₂ O=0 %	0.407	0.327	0.161	-359.93	-358.87	2.14	1.372	0.0154	0.0119	0.998	4.16
	5	0.411	0.332	0.158	-331	-329	2.96	1.343	0.0216	0.0232	0.996	3.81
	10	0.420	0.336	0.168	-321	-320	3.19	1.302	0.0239	0.0116	0.998	3.7
	15	0.442	0.339	0.205	-318	-315.1	3.24	1.249	0.0256	0.0336	0.995	3.66
	20	0.479	0.342	0.273	-300	-295	3.91	1.194	0.0317	0.0579	0.991	3.42
	25	0.509	0.347	0.324	-295.12	-290.77	3.98	1.159	0.0332	0.0504	0.993	3.37
	30	0.536	0.343	0.386	-282	-277.66	4.16	1.039	0.0385	0.0848	0.987	3.22
Series 2	V ₂ O ₅ =40 %	0.585	0.327	0.516	-196.32	-193.21	8.17	0.763	0.096	0.0361	0.994	2.239
	45	0.572	0.337	0.469	-220	-215.93	7.90	0.966	0.0756	0.0472	0.993	2.503
	50	0.556	0.340	0.431	-246	-242	6.88	1.139	0.0570	0.0464	0.993	2.806
	55	0.522	0.336	0.372	-273.3	-271.05	5.36	1.242	0.0414	0.0261	0.996	3.142
	60	0.512	0.333	0.358	-295	-291.6	4.67	1.371	0.0329	0.0394	0.994	3.381
	65	0.501	0.327	0.349	-318.44	-316.9	3.56	1.461	0.0238	0.0221	0.997	3.714
	70	0.459	0.321	0.277	-333	-328.95	3.39	1.538	0.0216	0.0470	0.993	3.814
Series 3	75	0.451	0.315	0.273	-360.13	-356.98	2.59	1.623	0.0157	0.0365	0.994	4.139
	Fe ₂ O ₃ =5 %	0.410	0.343	0.135	-333	-331	2.58	1.20	0.0207	0.0232	0.997	3.837
	7.5	0.431	0.334	0.195	-328.04	-324.6	2.79	1.20	0.0226	0.0397	0.994	3.764
	10	0.455	0.327	0.256	-319	-315	3.03	1.17	0.0252	0.0463	0.993	3.652
	12.5	0.496	0.319	0.354	-311	-306	3.20	1.11	0.0279	0.0579	0.991	3.548
15	0.506	0.313	0.387	-302	-296	3.40	1.05	0.0313	0.0695	0.989	3.432	

α' can be calculated from the intercept of this line. Figures 6.33 (a), (b) & (c) show the relation between thermoelectric power, Q , and $\ln(C_v/1-C_v)$. The slopes of this line are found to be $-81.92 \mu\text{V}/^\circ\text{K}$, $-85.324 \mu\text{V}/^\circ\text{K}$ and $-78.184 \mu\text{V}/^\circ\text{K}$ for series 1,2 and 3 respectively, which are close to the theoretical value of Heikes formula i.e., $-86.18 \mu\text{V}/^\circ\text{K}$. Mori et.al.^[6] reported the slopes $-86.60 \mu\text{V}/^\circ\text{K}$ and $-89.00 \mu\text{V}/^\circ\text{K}$ for $\text{V}_2\text{O}_5\text{-Sb}_2\text{O}_3\text{-TeO}_2$ and $\text{V}_2\text{O}_5\text{-Bi}_2\text{O}_3\text{-TeO}_2$ glasses respectively. Values of α' calculated from intercept of the line between Q and $\ln(C_v/1-C_v)$ are 0.228, 0.072 and 0.367 respectively for all three glass series.

According Austin and Mott^[14], α' term is assumed as zero if the disorder energy in the system is zero. Hence, thermoelectric power, Q , can also be calculated by using the values of C_v assuming α' equal to zero. The calculated values of Q_{cal} , therefore, are dependent on the accuracy of the measured value of C_v . The values of C_v were determined by the chemical analysis using photometric titration^[7] (Chapter 3.6). The calculated values of thermoelectric power, Q , are given in the Table 6.31. In the first glass series, the amount of V_2O_5 decreases with increasing amount of K_2O , which thereby increases the active reduced vanadium ions and increases the thermoelectric power Q , whereas, in glass series 2, with the increase of V_2O_5 , a decrease in the active reduced vanadium ions has been observed which thereby decreases the thermoelectric power Q . In glass series 3, the amount of both K_2O and Fe_2O_3 are increasing whereas, V_2O_5 is decreasing. The observed increase of thermoelectric power Q is comparatively smaller than those observed for glasses in series 1. This may be due to a very small decrease in the amount of V_2O_5 and iron is not present in reduced active state in glass series 3. However, the measured value of thermoelectric power is very close to the calculated values of Q , which may have an error of less than 2% because maximum error of 5 % in measurement of C_v , which is however, less than 5 % in the present case, will cause negligible error in Q_{cal} for these glasses. It has been observed that the values of Q_{cal} are slightly lower than that of the experimental values of

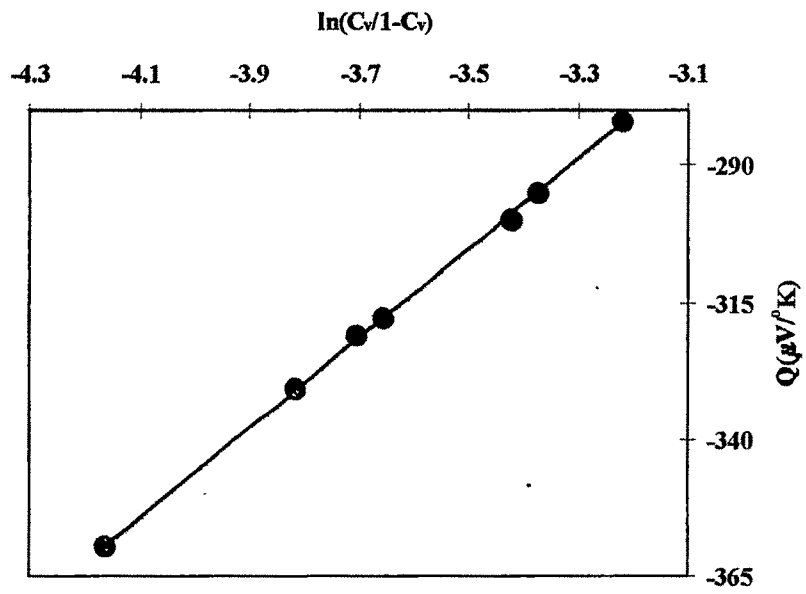


Figure 6.33 (a) : Plot of $Q (\mu V/K)$ versus $\ln(C_v/1-C_v)$ for series 1.

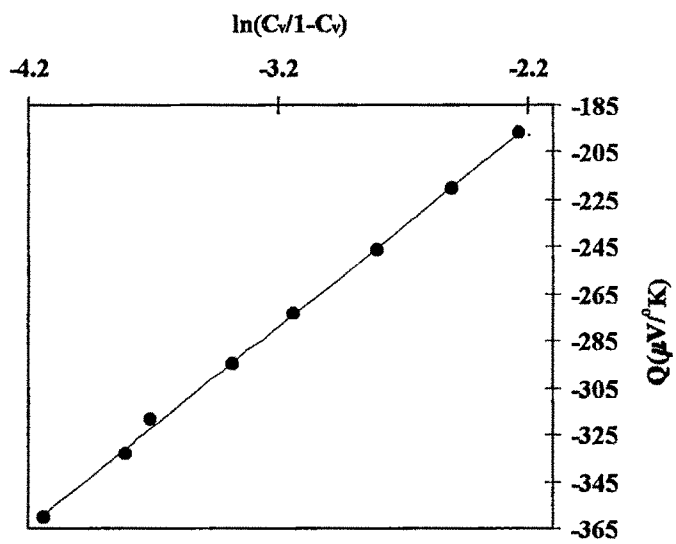


Figure 6.33 (b): Plot of $Q(\mu V/K)$ versus $\ln(C_v/1-C_v)$ for series 2.

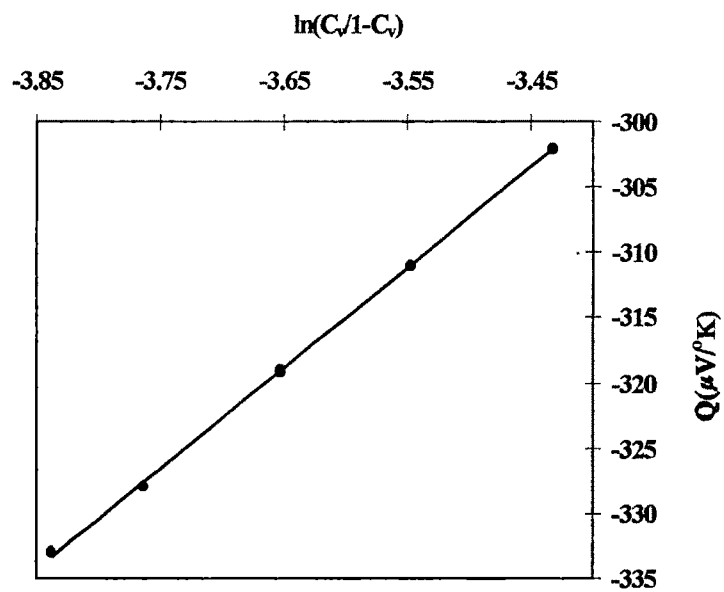


Figure 6.33 (c): Plot of Q ($\mu\text{V}/\text{K}$) versus $\ln(C_v/1-C_v)$ for series 3.

Q. The difference between measured value of Q and Q_{cal} are given in Table 6.31. As these difference is observed to be ~3 to 4 % for all the glasses. Hence, α' cannot be neglected in the discussion of these glasses. The values of α' for all glasses lies in the range of 0.01194 to 0.0848, 0.0221 to 0.0472 and 0.0232 to 0.0695 in series 1, 2 and 3 respectively. It may be noticed from the Table 6.31 that a slight increase in α' is observed with increasing concentration of K_2O in series 1. However in glass series 2, the increase in the amount of V_2O_5 , the values of α' should decrease, but it is observed from the Table 6.31 that the values of α' does not show much variations.

Incase of glass series 3, an increase of α' is observed (Table 6.31) with corresponding increase in Fe_2O_3 , which can be interpreted as an increase in active reduced valence sites (V^{+4}). An increase in active reduced valence sites will increase the effective value of C_v (i.e. V^{+4}/V_{total}), thereby decreasing the concentration of $\ln(C_v/1-C_v)$ and increase the value of α' [5]. At the same time, the values of α' which are much less than unity, satisfy the condition for small polaron formation in these glasses. As the value of α' are not zero i.e. α' is finite, the values of θ , a measure of disorderness in the system have been calculated using Equation^[11,14],

$$\alpha' = \left(\frac{W_H}{kT} \right) \left[\frac{1-\theta}{1+\theta} \right] \quad (6.32)$$

where W_H is the activation energy for hopping whose values are mentioned in the Table 6.31. k is the Boltzmann's constant. As it is well established that, a deviation of values of θ from unity is a measure of disorder in the system [14]. The value of θ different from unity will provide α' value other than zero which inturn will contribute to the measured values of thermal power. In the present glass systems, the values of θ are observed to be less than unity but remains constant i.e., lies about 0.99 to 0.98 in all the samples (Table 6.31). These values, different from unity, are a measure of disorderness in the glass system. Hence, the disorder energy, W_D , has been calculated from

$$W_D = 2(W - W_H) \quad (6.33)$$

where, W is the activation energy and W_H , the hopping energy. The disorder energy, W_D , varies from 0.161 eV to 0.386 eV, 0.516 eV to 0.273 eV and 0.135 eV to 0.387 eV in series 1, 2 and 3 respectively. Because of the formation of small polarons, all the site may not participate in conduction process, hence increase in W_D with decrease of V_2O_5 is expected in the present glass systems. In the case of series 1, the amount of glass modifier K_2O is increasing which results an increase of disorderness in the system and hence increase the disorder energy^[18], whereas the increase of V_2O_5 glass former in the second series is responsible for decreasing the disorder energy. Moreover, B_2O_3 which has better glass forming ability than V_2O_5 decreases in this glass series, and consequently decreases the disorder energy W_D :

In glass series 3, an increase in the amount of glass modifier K_2O and Fe_2O_3 with decreasing amount of V_2O_5 is responsible for increase of disorder in the system which in turn increases the disorder energy W_D .

It is evident from Equation 6.32 that α' should be dependent on temperature, hence, thermoelectric power, Q , too is expected to be dependent on temperature^[17]. As the values of α' are very small ($\alpha' \ll 1$), Q can be expected to be temperature independent, which is observed in the present glass systems.

Apart from Heikes formula^[11,12], Mackenzie^[3,10] too proposed the following formula for semiconducting glasses with transition metal oxides for calculation of thermoelectric power Q .

$$Q = \left(\frac{k}{e} \right) \ln \left[\frac{\text{High Valence Ions}}{\text{Low Valence Ions}} \right] \quad (6.34)$$

where k is a Boltzmann constant and e is an electronic charge. In V_2O_5 based glasses, the term high valence ions/ Low valence ions is formally represented by V^{+5}/V^{+4} . Theoretically, the thermoelectric power, Q , of a glass containing V_2O_5 with hopping conduction ought to obey Equation 6.34, according to

which the thermoelectric power, Q , having ratio V^{+5}/V^{+4} greater than unity will be negative owing to the predominant hopping of electrons while, in highly reduced glasses where V^{+5}/V^{+4} is less than one, Q will be positive owing to predominant hopping of holes and if V^{+5}/V^{+4} equals to unity, i.e., when the hopping of electrons and holes takes place with equal probability, the Q will be zero^[7,19]. Allersma T. and Mackenzie J. D.^[3,10] have reported for V_2O_5 based glasses with $\ln(V^{+5}/V^{+4}) > 1$, the thermoelectric power, Q , becomes negative indicating n-type semiconductor but for $\ln(V^{+5}/V^{+4}) < 1$, Q is positive meaning p-type semiconductor. In the present glass series, the ratio $\ln(V^{+5}/V^{+4})$ lies in the range of 4.16 to 3.22, 4.139 to 2.239 and 3.837 to 3.432 for glass series 1, 2 and 3 respectively which are greater than unity indicating that all the glasses in the present study are of n-type semiconductor in nature. The slope calculated [Figures 6.34 (a), (b) & (c)] from the Mackenzie's formula (Equation 6.34) are $-81.920 \mu V/^{\circ}K$, $-85.324 \mu V/^{\circ}K$ and $-78.184 \mu V/^{\circ}K$ respectively for all three series, which are similar to the values obtained from Heikes formula^[11,12]. The ratio of high valence ions to low valence ions i.e., V^{+5}/V^{+4} is also very important for understanding the conduction mechanism in these glasses^[7,20]. A conduction mechanism of $GeO_2-P_4O_{10}-V_2O_5$ ^[20] revealed that the electronic conductivity of the glasses decreases rapidly with the decrease of ratio $\ln(V^{+5}/V^{+4})$ as the concentration of V_2O_5 increases. It is observed from Table 6.31 that the conductivity decreases with decrease of $\ln(V^{+5}/V^{+4})$ ratio for series 1 and 3, whereas the conductivity increases with increase of $\ln(V^{+5}/V^{+4})$ ratio in series 2 as the concentration of V_2O_5 increases. The activation energy of series 1 and 3 increases with the decrease of $\ln(V^{+5}/V^{+4})$ ratio whereas the activation energy decreases with the increase of $\ln(V^{+5}/V^{+4})$ ratios increase of V_2O_5 concentration^[7,20] in series 2 (Table 6.31). It not only confirms the n-type nature but also proves the applicability of Mackenzie formula to the present glass system.

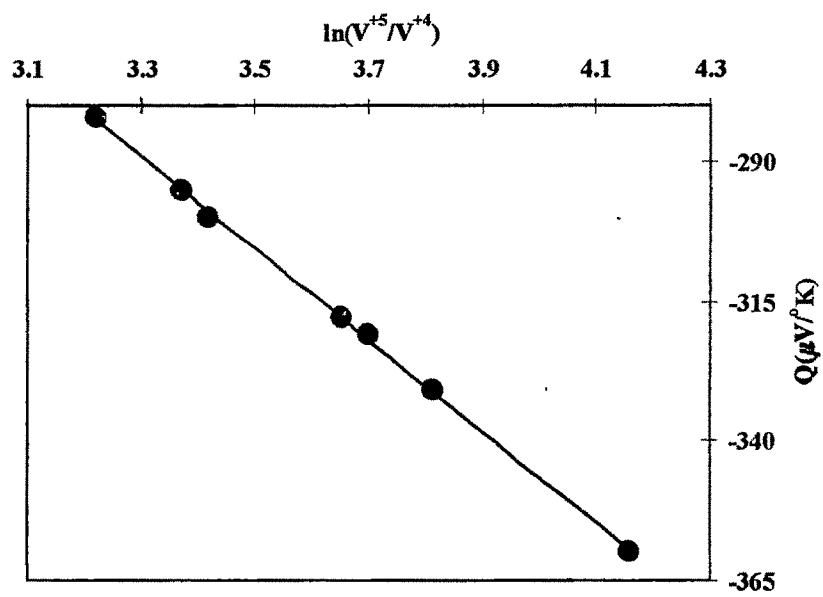


Figure 6.34 (a) : Plot of $Q(\mu V/K)$ versus $\ln(V^{+5}/V^{+4})$ for series 1.

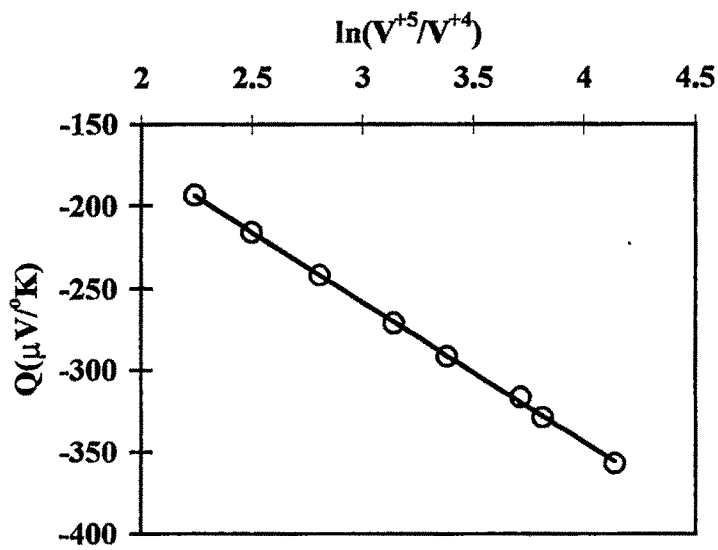


Figure 6.34 (b): Plot of $Q(\mu V/K)$ versus $\ln(V^{+5}/V^{+4})$ for series 2.

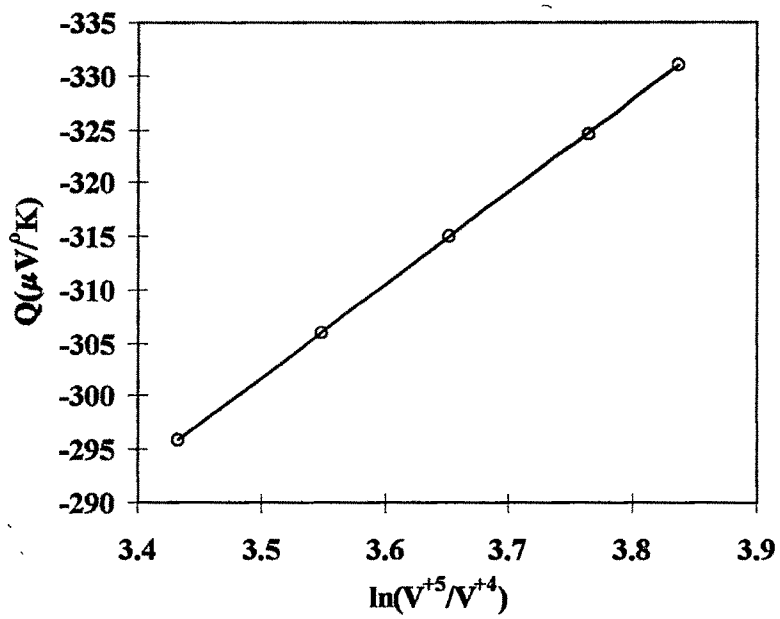


Figure 6.34 (c) : Plot of $Q(\mu V/K)$ versus $\ln(V^{+5}/V^{+4})$ for series 3.

REFERENCES:

1. A. P. Schmidt, *J. Appl. Phys.* 39(1968)3140.
2. N. F. Mott, *J. of Non-Cryst. Solids* 1(1968)1.
3. T. N. Kennedy & J. D. Mackenzie, *Phys. & Chem. Of Glasses*, 8(1967)169.
4. V. N. Bogomolov, E. K. Kudinov & Yu. A. Firsov, *Sov. Phys. Solid St.* 9(1968)2502.
5. A. Mansingh & A. Dhawan, *J. Phys. C, Solid State Physics*, Vol. 11(1978)3439.
6. H. More & H. Sakata, *J. of Mater. Sci.* 31(19996)1621.
7. Y. Kawamoto, M. Fukuzuka, Y. Ohta & M. Imai, *Phys. & Chem. Of Glasses*, Vol. 20, No. 3(1979)54.
8. D. K. Kanchan & H. R. Panchal, *Solid State Physics (India)*, Vol. 41(1998)256.
9. A. Ghosh, *J. of Appl Phys.*, 65(1989)227.
10. T. Allersma & J. D. Mackenzie, *J. Chem. Phys.*, 47(1967)1406.
11. R. R. Heikes, A. A. Mardudin & R. C. Miller, *Ann. Phys. N.Y.*, 8(1963)733.
12. R. R. Heikes, "Thermoelectricity" edited by R. R. Heikes & R. W. Ure (Interscience NY, 1961)p. 81.
13. J. Appel, *Solid State Physics*, 21(1968)193.
14. I. G. Austin & N. F. Mott, *Adv. Phys.* 18(1969)41.
15. G. L. Sewell, *Phys. Rev.* 129(1963)597.
16. M. I. Klinger, *Rep. Prog. Phys.* 30(1968)225.
17. Lynch G. F., M. Sayer, S. L. Segel and Rosenblatt. *J. Appl. Phys.* 42(1971)2587.
18. H. R. Panchal, D. K. Kanchan & D. R. Somayajulu, *J. of Mater. Sci. Forum*, Vol. 223-224(1996)301.

19. G. S. Linsley, A. E. Owen, F. M. Haytee, *J. of Non-Cryst. Solids* 4(1970)208.
20. Janmakirama Rao BH. V., *J. of Amm. Cerm. Soc.* Vol. 48, No. 6, (1965)311.